Springer

Dear Author,

Here are the proofs of your article.

- You can submit your corrections **online**, via **e-mail** or by **fax**.
- For **online** submission please insert your corrections in the online correction form. Always indicate the line number to which the correction refers.
- You can also insert your corrections in the proof PDF and **email** the annotated PDF.
- For fax submission, please ensure that your corrections are clearly legible. Use a fine black pen and write the correction in the margin, not too close to the edge of the page.
- Remember to note the **journal title**, **article number**, and **your name** when sending your response via e-mail or fax.
- **Check** the metadata sheet to make sure that the header information, especially author names and the corresponding affiliations are correctly shown.
- **Check** the questions that may have arisen during copy editing and insert your answers/ corrections.
- **Check** that the text is complete and that all figures, tables and their legends are included. Also check the accuracy of special characters, equations, and electronic supplementary material if applicable. If necessary refer to the *Edited manuscript*.
- The publication of inaccurate data such as dosages and units can have serious consequences. Please take particular care that all such details are correct.
- Please **do not** make changes that involve only matters of style. We have generally introduced forms that follow the journal's style.
  Substantial changes in content, e.g., new results, corrected values, title and authorship are not allowed without the approval of the responsible editor. In such a case, please contact the Editorial Office and return his/her consent together with the proof.
- If we do not receive your corrections **within 48 hours**, we will send you a reminder.
- Your article will be published **Online First** approximately one week after receipt of your corrected proofs. This is the **official first publication** citable with the DOI. **Further changes are, therefore, not possible.**
- The **printed version** will follow in a forthcoming issue.

Please note

After online publication, subscribers (personal/institutional) to this journal will have access to the complete article via the DOI using the URL: http://dx.doi.org/[DOI].
If you would like to know when your article has been published online, take advantage of our free alert service. For registration and further information go to: http://www.link.springer.com.

Due to the electronic nature of the procedure, the manuscript and the original figures will only be returned to you on special request. When you return your corrections, please inform us if you would like to have these documents returned.

Metadata of the article that will be visualized in OnlineFirst

ArticleTitle	Combined Gravimetric–Seismic Crustal Model for Antarctica	
Article Sub-Title		
Article CopyRight	Springer Science+Business Media B.V. (This will be the copyright line in the final PDF)	
Journal Name	Surveys in Geophysics	
Corresponding Author	Family Name	**Tenzer**
	Particle	
	Given Name	**Robert**
	Suffix	
	Division	Department of Land Surveying and Geo-Informatics
	Organization	Hong Kong Polytechnic University
	Address	Kowloon, Hong Kong
	Phone	
	Fax	
	Email	robert.tenzer@polyu.edu.hk
	URL	
	ORCID	
Author	Family Name	**Baranov**
	Particle	
	Given Name	**Alexey**
	Suffix	
	Division	Schmidt Institute of Physics of the Earth
	Organization	Russian Academy of Sciences
	Address	Moscow, Russian Federation
	Division	Institute of Earthquake Prediction Theory and Mathematical Geophysics
	Organization	Russian Academy of Sciences
	Address	Moscow, Russian Federation
	Phone	
	Fax	
	Email	
	URL	
	ORCID	
Author	Family Name	**Bagherbandi**
	Particle	
	Given Name	**Mohammad**
	Suffix	
	Division	Division of Geodesy and Geoinformatics
	Organization	Royal Institute of Technology (KTH)
	Address	Stockholm, Sweden
	Division	Department of Industrial Development, IT and Land Management

Organization	University of Gävle
Address	Gävle, Sweden
Phone	
Fax	
Email	
URL	
ORCID	

	Received	11 May 2017
Schedule	Revised	
	Accepted	8 August 2017

Abstract

The latest seismic data and improved information about the subglacial bedrock relief are used in this study to estimate the sediment and crustal thickness under the Antarctic continent. Since large parts of Antarctica are not yet covered by seismic surveys, the gravity and crustal structure models are used to interpolate the Moho information where seismic data are missing. The gravity information is also extended offshore to detect the Moho under continental margins and neighboring oceanic crust. The processing strategy involves the solution to the Vening Meinesz-Moritz's inverse problem of isostasy constrained on seismic data. A comparison of our new results with existing studies indicates a substantial improvement in the sediment and crustal models. The seismic data analysis shows significant sediment accumulations in Antarctica, with broad sedimentary basins. According to our result, the maximum sediment thickness in Antarctica is about 15 km under Filchner-Ronne Ice Shelf. The Moho relief closely resembles major geological and tectonic features. A rather thick continental crust of East Antarctic Craton is separated from a complex geological/tectonic structure of West Antarctica by the Transantarctic Mountains. The average Moho depth of 34.1 km under the Antarctic continent slightly differs from previous estimates. A maximum Moho deepening of 58.2 km under the Gamburtsev Subglacial Mountains in East Antarctica confirmed the presence of deep and compact orogenic roots. Another large Moho depth in East Antarctica is detected under Dronning Maud Land with two orogenic roots under Wohlthat Massif (48–50 km) and the Kottas Mountains (48–50 km) that are separated by a relatively thin crust along Jutulstraumen Rift. The Moho depth under central parts of the Transantarctic Mountains reaches 46 km. The maximum Moho deepening (34–38 km) in West Antarctica is under the Antarctic Peninsula. The Moho depth minima in East Antarctica are found under the Lambert Trench (24–28 km), while in West Antarctica the Moho depth minima are along the West Antarctic Rift System under the Bentley depression (20–22 km) and Ross Sea Ice Shelf (16–24 km). The gravimetric result confirmed a maximum extension of the Antarctic continental margins under the Ross Sea Embayment and the Weddell Sea Embayment with an extremely thin continental crust (10–20 km).

Keywords (separated by '-'): Antarctica - Crust - Gravity - Ice - Isostasy - Moho - Sediments - Seismic data

Footnote Information

Journal : Small 10712 | Dispatch : 11-8-2017 | Pages : 34
Article No. : 9423 | ☐ LE | ☐ TYPESET
MS Code : GEOP-D-17-00046 | ✔ CP | ✔ DISK

Surv Geophys
DOI 10.1007/s10712-017-9423-5

CrossMark

Combined Gravimetric–Seismic Crustal Model for Antarctica

Alexey Baranov[1,2] · Robert Tenzer[3] · Mohammad Bagherbandi[4,5]

Received: 11 May 2017 / Accepted: 8 August 2017

Abstract The latest seismic data and improved information about the subglacial bedrock relief are used in this study to estimate the sediment and crustal thickness under the Antarctic continent. Since large parts of Antarctica are not yet covered by seismic surveys, the gravity and crustal structure models are used to interpolate the Moho information where seismic data are missing. The gravity information is also extended offshore to detect the Moho under continental margins and neighboring oceanic crust. The processing strategy involves the solution to the Vening Meinesz-Moritz's inverse problem of isostasy constrained on seismic data. A comparison of our new results with existing studies indicates a substantial improvement in the sediment and crustal models. The seismic data analysis shows significant sediment accumulations in Antarctica, with broad sedimentary basins. According to our result, the maximum sediment thickness in Antarctica is about 15 km under Filchner-Ronne Ice Shelf. The Moho relief closely resembles major geological and tectonic features. A rather thick continental crust of East Antarctic Craton is separated from a complex geological/tectonic structure of West Antarctica by the Transantarctic Mountains. The average Moho depth of 34.1 km under the Antarctic continent slightly differs from previous estimates. A maximum Moho deepening of 58.2 km under the Gamburtsev Subglacial Mountains in East Antarctica confirmed the presence of

✉ Robert Tenzer
robert.tenzer@polyu.edu.hk

[1] Schmidt Institute of Physics of the Earth, Russian Academy of Sciences, Moscow, Russian Federation

[2] Institute of Earthquake Prediction Theory and Mathematical Geophysics, Russian Academy of Sciences, Moscow, Russian Federation

[3] Department of Land Surveying and Geo-Informatics, Hong Kong Polytechnic University, Kowloon, Hong Kong

[4] Division of Geodesy and Geoinformatics, Royal Institute of Technology (KTH), Stockholm, Sweden

[5] Department of Industrial Development, IT and Land Management, University of Gävle, Gävle, Sweden

Journal : Small 10712 Dispatch : 11-8-2017 Pages : 34
Article No. : 9423 LE TYPESET
MS Code : GEOP-D-17-00046 CP DISK

deep and compact orogenic roots. Another large Moho depth in East Antarctica is detected under Dronning Maud Land with two orogenic roots under Wohlthat Massif (48–50 km) and the Kottas Mountains (48–50 km) that are separated by a relatively thin crust along Jutulstraumen Rift. The Moho depth under central parts of the Transantarctic Mountains reaches 46 km. The maximum Moho deepening (34–38 km) in West Antarctica is under the Antarctic Peninsula. The Moho depth minima in East Antarctica are found under the Lambert Trench (24–28 km), while in West Antarctica the Moho depth minima are along the West Antarctic Rift System under the Bentley depression (20–22 km) and Ross Sea Ice Shelf (16–24 km). The gravimetric result confirmed a maximum extension of the Antarctic continental margins under the Ross Sea Embayment and the Weddell Sea Embayment with an extremely thin continental crust (10–20 km).

Keywords Antarctica · Crust · Gravity · Ice · Isostasy · Moho · Sediments · Seismic data

1 Introduction

A pioneering study of the Antarctic crustal structure can be attributed to Evison et al. (1960). They estimated, based on the analysis of surface wave dispersion, that the crustal thickness in East Antarctica and Marie Byrd Land is around 35 and 25 km, respectively. Regional studies of surface wave velocities were conducted by Kovach and Press (1961), Bentley and Ostenso (1962), Dewart and Toksoz (1965), Adams (1971), Knopoff and Vane (1978), Rouland et al. (1985), Forsyth et al. (1987), Roult et al. (1994), Bannister et al. (2003), and others. Deep seismic sounding profiles were carried out by Kogan (1972), Kolmakov et al. (1975), Fedorov et al. (1982), and Ito and Ikami (1986). Kogan (1972) and Ito and Ikami (1986) used localized controlled source seismic experiments. A seismic receiver function analysis was carried out by Winberry and Anandakrishnan (2004), Reading (2006), Lawrence et al. (2006), Hansen et al. (2009), Chaput et al. (2014), and Ramirez et al. (2016). Since a lack of intraplate seismicity in Antarctica (e.g., Okal 1981), passive seismic studies of earthquakes occurring mostly outside the Antarctic tectonic plate also represent a significant source of information about the Antarctic crustal structure. Nevertheless, the current knowledge about the Antarctic geological and tectonic structure is still limited due to a low spatial coverage of high-quality seismic data. Some authors, therefore, used the gravity, topographic, and ice thickness information to predict the crustal thickness in Antarctica. von Frese et al. (1999), for instance, estimated an average crustal thickness from 35 to 45 km across East Antarctica based on the analysis of the surface topography and ice thickness measurements from the BEDMAP1 project (Lythe et al. 2001). Studinger et al. (2004, 2006) used results from airborne gravity surveys to study the crustal structure in parts of Antarctica.

 The first (continental-scale) Antarctic crustal models were published by Bentley (1991) and Groushinsky et al. (1992). They derived the Moho depth from several deep seismic sounding profiles including gravity data, while interpolating information across wide data gaps. According to their results, the Moho depth varies typically between 25 and 30 km along coastal margins, and deepens to about 50 km in central parts of East Antarctica. Ritzwoller et al. (2001) used the simultaneous inversion of broadband group velocity measurements to compile a seismic model of the crust and the upper mantle beneath Antarctica and surrounding oceans. Llubes et al. (2003) estimated the crustal thickness in Antarctica using the CHAMP satellite-derived gravity data (Reigber et al. 2002). Block

Journal : Small 10712 | Dispatch : 11-8-2017 | Pages : 34
Article No. : 9423 | LE | TYPESET
MS Code : GEOP-D-17-00046 | CP | DISK

et al. (2009) estimated the crustal thickness from the GRACE satellite gravity data (Tapley et al. 2004). Jordan et al. (2010) estimated the Moho depth for West Antarctica from the aero-gravity and aeromagnetic data. They identified a thin crust (18–20 km) under Pine Island Glacier, Bentley Trench, and Byrd Subglacial Basin, whereas the Moho depth under the Ellsworth Mountains is about 35 km. Ferraccioli et al. (2011) found a thickened continental crust under the Gamburtsev Mountains (45–58 km). Moreover, the neighboring Precambrian provinces have a normal (Prince Charles Mountains) or thinned (Lambert Rift) continental crust. Jordan et al. (2013) investigated the crustal structure of the Wilkes Subglacial Basin using airborne gravity data. They estimated that the crustal thickness under the northern and southern parts of Wilkes Subglacial Basin is about 30 and 35 km, respectively.

Baranov and Morelli (2013) compiled the seismic Antarctic Moho model (ANTMoho) based on the analysis of seismic experiments, receiver functions, and available geological evidence. They identified three distinctive features in the Antarctic Moho relief, comprising the oldest Archean and Proterozoic crust of East Antarctica with the Moho depth between 36 and 56 km (with an average of about 41 km), the continental crust of the Transantarctic Mountains including the Antarctic Peninsula and Wilkes Basin with the Moho depth typically from 30 to 40 km (with an average of about 30 km), and the youngest rifted continental crust of the West Antarctic Rift System with the Moho depth ranging from 16 to 28 km (with an average of about 26 km). According to their estimates, the average Moho depth for the whole Antarctic continent is 33.8 km. Chaput et al. (2014) further improved the current knowledge about the crustal thickness across West Antarctica, including the West Antarctic Rift System, Marie Byrd Land dome, and the Transantarctic Mountains margin. They used the P-to-S receiver functions from seismographic stations of the POLENET-ANET project (the West Antarctic and Transantarctic Mountains portion of the Polar Earth Observing Network) that was funded as a part of the International Polar Year (IPY). According to their estimates, the crustal thickness in that region varies from 17.0 ± 4 km at Fishtail Point in the western part of the West Antarctic Rift System to 45 ± 5 km at Lonewolf Nunataks in the Transantarctic Mountains. In the most recent study, O'Donnell and Nyblade (2014) presented a continental-scale crustal thickness model for Antarctica, derived from the GOCO03S global gravitational model (Mayer-Gürr et al. 2012) and constrained on the seismic crust thickness estimates. They reported an average crustal thickness of about 40 km for East Antarctica (a value typical for continental shields) and 24 km for West Antarctica. They also estimated locally a significant Moho deepening (exceeding 50 km) beneath the Gamburtsev Subglacial Mountains, the Vostok Highlands, and parts of the Transantarctic Mountains and Dronning Maud Land. The Moho depth for other regions of East Antarctica (Enderby Land, Aurora Basin, and Wilkes Subglacial Basin) is typically about 40 km. They found the deepest Moho in West Antarctica (29–34 km) under Marie Byrd Land, the Ellsworth–Whitmore Mountains and part of Antarctic Peninsula, whereas for other regions of West Antarctica, the Moho depth is about 23–27 km with an extreme continental crustal extension under the Ross Sea and Weddell Sea Embayment. An et al. (2015) compiled a regional crustal model using data from 122 broadband seismic stations and about 10,000 Rayleigh waves. They reported a thick crust under the East Antarctic Mountain Ranges with a maximum Moho deepening under the Gamburtsev Mountains (about 60 km). They also estimated a rather thin crust (about 25 km) in West Antarctica with thinnest crust under Ross Ice Shelf and an intermediate crust (30–45 km) under the Transantarctic Mountains.

In the absence of seismic data, gravimetric methods are often applied to detect the Moho interface based on adopting a particular hypothesis about an isostatic mass balance.

Journal : Small 10712 Dispatch : 11-8-2017 Pages : 34
Article No. : 9423 □ LE □ TYPESET
MS Code : GEOP-D-17-00046 ✔ CP ✔ DISK

Pratt's (1855) theory assumed a variable density of compensation, while Airy's (1885) theory was based on assuming a variable depth of compensation. Both these isostatic models assume only a local compensation mechanism. Vening Meinesz (1931) modified Airy's theory by introducing a regional compensation scheme for a thin plate lithospheric flexure model. A regional compensation model was later utilized also in Parker–Oldenburg's isostatic method (Parker 1972; Oldenburg 1974) by assuming a variable crustal thickness, while adopting a uniform Moho density contrast. Parker–Oldenburg's method was presented for a planar approximation and solved by applying the fast Fourier transform (FFT) technique. Moritz (1990) generalized Vening Meinesz's inverse problem for a global compensation mechanism and a spherical approximation of the Earth. Later, Sjöberg (2009) reformulated Moritz's problem, called Vening Meinesz-Moritz's inverse problem of isostasy, as that of solving (nonlinear) Fredholm's integral equation of the first kind. The solutions by Moritz (1990) and Sjöberg (2009) use the same idea, but the former (and also Parker–Oldenburg's method) applies an iterative approach, while the latter provides a direct solution.

Following the latest update on ice thickness and seismic data, we used the BEDMAP2 subglacial relief (Fretwell et al. 2013) and results from the analysis of teleseismic receiver functions, seismic reflection, and refraction data (Baranov and Morelli 2013), including results from processing the POLENET-ANET receiver functions (Chaput et al. 2014) to compile a new seismic Moho model for the Antarctic continent. We further used these seismic data to provide new estimates of the continental sediment thickness. Since seismic data in Antarctica are still sparse and irregularly distributed, we used the gravity and crustal structure models to interpolate the Moho information in regions where seismic data are missing. In existing studies investigating the Moho interface under Antarctica, isostatic models were applied based on assuming a local compensation mechanism and adopting a planar approximation. Llubes et al. (2003), for instance, estimated the crustal thickness in Antarctica based on applying a simple linear relation between the crustal thickness and the planar Bouguer gravity reduction. Block et al. (2009) derived the crustal thickness from gravity data based on applying Parker–Oldenburg's method, and O'Donnell and Nyblade (2014) derived the Antarctic crustal thickness from the gravity and topographic models according to Airy's theory. To determine the Moho depth in Antarctica from gravity data more realistically, we applied in this study Vening Meinesz-Moritz's isostatic scheme. As demonstrated by Eshagh (2016), the Moho depth differences between values obtained based on applying Airy and Vening Meinesz-Moritz's isostatic schemes reach several kilometers. The isostatic gravity data we used for a gravimetric Moho recovery were evaluated from the GOCO05S gravitational model (Mayer-Gürr et al. 2015) and the ETOPO1 topographic/bathymetric data (Amante and Eakins 2009). Since most of Antarctica is covered by continental glaciers (Fig. 2b), we applied the ice stripping gravity correction that was computed from the BEDMAP2 ice thickness data. We further applied the sediment stripping gravity correction and computed from the CRUST1.0 global sediment dataset (Laske et al. 2013), which we regionally updated according to our new sediment model for the Antarctic continent. Furthermore, we adopted the density model of marine sediments developed by Tenzer and Gladkikh (2014) to evaluate the gravitational contribution of marine sediment deposits.

A subsequent part of the article begins with a summary of the Antarctic geological and tectonic setting in Sect. 2. Results of seismic data analysis are presented in Sect. 3, and gravimetric results are shown in Sect. 4. The combined (gravimetric–seismic) Moho model for Antarctica is compiled in Sect. 5, and then compared with the gravimetric and seismic

Journal : Small 10712 | Dispatch : 11-8-2017 | Pages : 34
Article No. : 9423 | ☐ LE | ☐ TYPESET
MS Code : GEOP-D-17-00046 | ☑ CP | ☑ DISK

models in Sect. 6. Uncertainties of estimated Moho models and the results are discussed in Sects. 7 and 8, and major findings are given in Sect. 9.

2 Antarctic Geological and Tectonic Setting

The Antarctic tectonic plate was formed around 35 Myr ago after breakup from Gondwana and moving south to its present isolated polar location that has led to a development of the present-day hyper-arid, cold polar climate (Stonehouse 2002). The Antarctic plate (extending over an area of 60×10^6 km^2) is bounded almost entirely by the extensional mid-oceanic ridge systems and bordered with the Nazca, South American, Somali, African, Australian, Pacific, and Juan Fernandez adjacent plates, the Scotia plate across a transform boundary including the Sandwich and Shetland (micro)plates (Fig. 1). A prevailing horizontal motion of the Antarctic plate was estimated to be at least 1 cm/year toward the Atlantic Ocean.

The Antarctic continent (extending over an area of 14×10^6 km^2) is almost entirely covered by continental glaciers (about 99%) with a maximum thickness reaching 4.6 km (see Fig. 2b) and an average thickness of 1.94 km (cf. Fretwell et al. 2013). The subglacial relief is very complex and ranges from −2.5 to 4.0 km (Fig. 2a). The maximum topographic elevations reach 4.9 km (Mt. Vinson). The three largest mountain ranges on the Antarctic continent are the Transantarctic Mountains and the West and East Antarctica ranges (Bentley 1991).

The Antarctic plate formation to its present stage involved major geological episodes throughout the Proterozoic Eon, Paleozoic, Mesozoic, and Cenozoic periods. The Grunehogna, Napier, and Mawson cratons of East Antarctica preserved the evidence of tectonic activity from the Archean (Baranov and Bobrov 2017, in press). The initial breakup between Australia, India, and Antarctica occurred in the Early Cretaceous. The Late Cretaceous was characterized by the main phase of extensional tectonism between

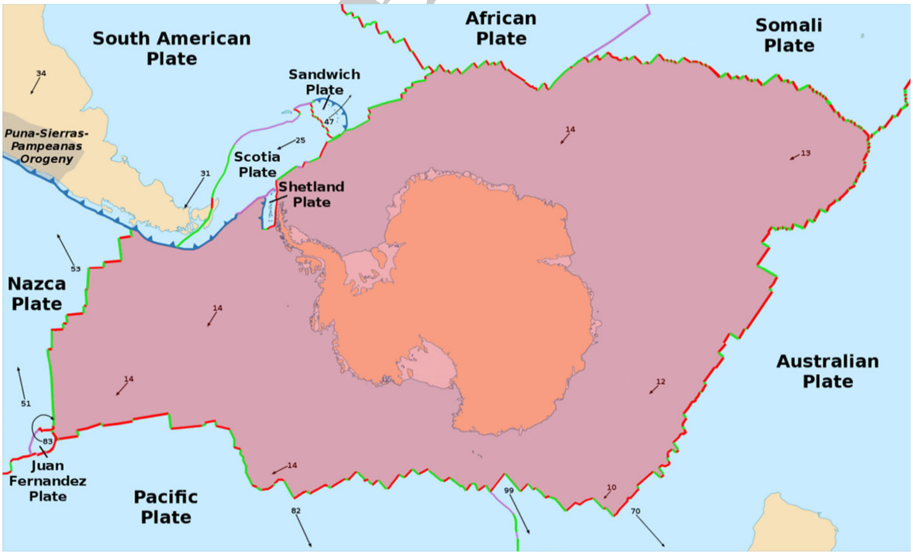

Fig. 1 Antarctic tectonic plate configuration retrieved from the updated tectonic map of Bird (2003)

Journal : Small 10712 Dispatch : 11-8-2017 Pages : 34
Article No. : 9423 LE TYPESET
MS Code : GEOP-D-17-00046 CP DISK

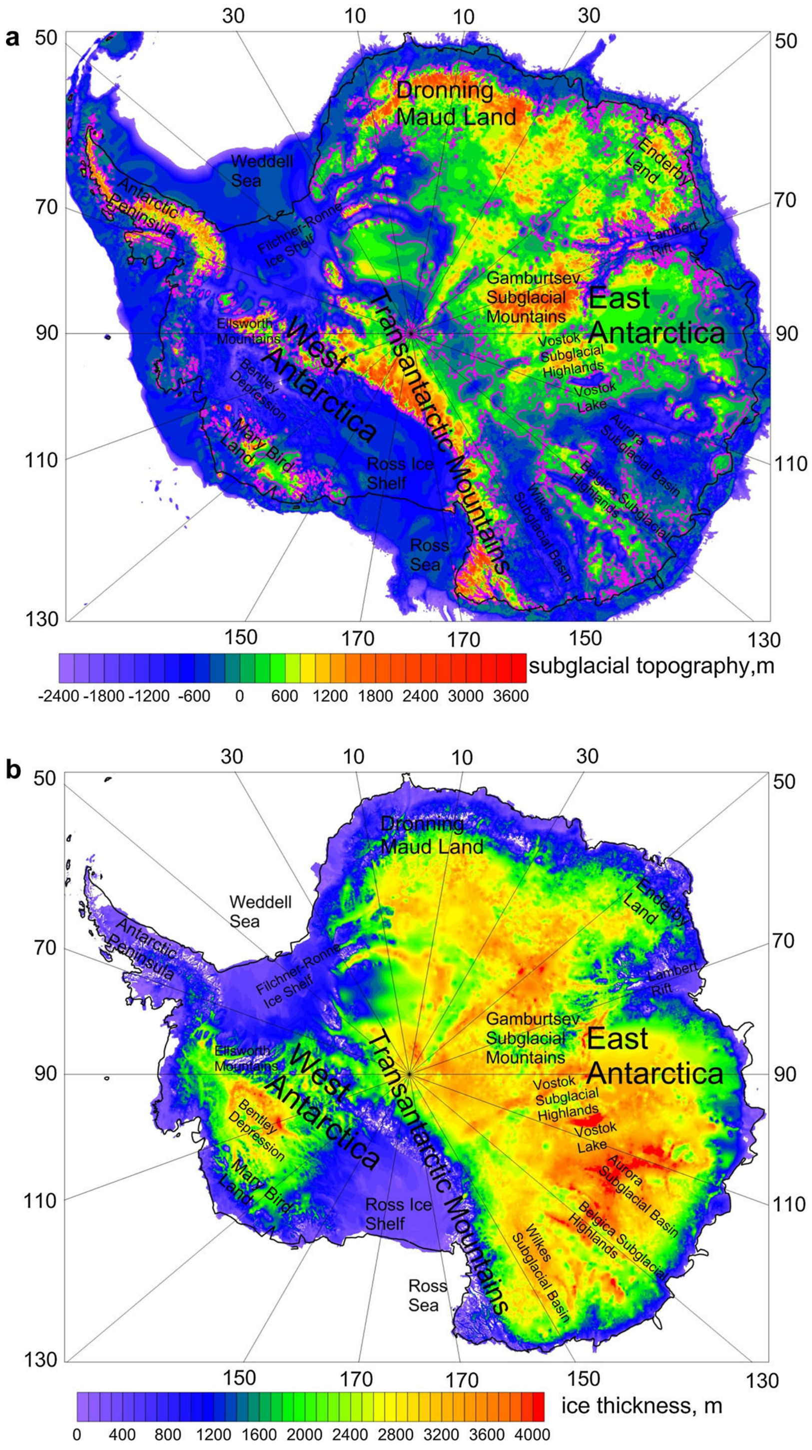

Fig. 2 Regional maps of: **a** bedrock topography and **b** ice thickness

Journal : Small 10712 Dispatch : 11-8-2017 Pages : 34
Article No. : 9423 LE TYPESET
MS Code : GEOP-D-17-00046 CP DISK

East and West Antarctica. The propagation southward of seafloor spreading from the Adare Trough into the continental crust underlying the western Ross Sea in the Early Cenozoic, likely caused a flexural uplift of the East Antarctic lithosphere, followed by a formation of the Transantarctic Mountains.

Geology of East and West Antarctica are quite different. Whereas West Antarctica is composed by an assemblage of Mesozoic and Cenozoic accreted terranes, East Antarctica is formed mainly by a Precambrian stable continental craton (Dalziel and Elliot 1982; Dalziel 1992). Tectonic processes from the Late Cretaceous onwards have been dominated by the uplift and rifting between West and East Antarctica along what is now known as the West Antarctic Rift System, which represents one of the largest continental extensional zones consisting of accreted terranes (Wörner 1999). The subglacial relief map of West Antarctica (Fretwell et al. 2013) revealed significant variations consisting of deep trenches (Bentley Trench) and elevated topography (Ellsworth Mountains and Antarctic Peninsula). The Ross Sea is a part of the West Antarctic Rift System, a crustal rift between the Transantarctic Mountains and the uplifted area of Marie Byrd Land (Behrendt et al. 1991). Subglacial topographic features comprise also three major sedimentary basins, namely the Victoria Land Basin, the Central Basin, and the Eastern Basin, that are separated by the Coulman High and the Central High (Trey et al. 1999). Marie Byrd Land, located east of the Ross Ice Shelf and the Ross Sea, is a large intraplate volcanic province (Hole and LeMasurier 1994). The opening of the West Antarctic Rift is closely related to the uplift and formation of the Transantarctic Mountains that begun in the Early Cenozoic. The Transantarctic Mountains are the largest non-collisional mountains in the world (ten Brink et al. 1997), with no evidence of a compressional origin, and thus different from most mountain ranges of a similar size (Studinger et al. 2004). West Antarctica is formed by a number of relatively small plate fragments that have been merged together along the southeastern Pacific compressional plate boundary. The most significant among them are the Ross Sea and Ross Ice Shelf region, Marie Byrd Land with the Bentley Trench, the Ellsworth–Whitmore Mountains, the Antarctic Peninsula, and the Filchner-Ronne Ice Shelf with the Weddell Sea (Dalziel and Elliot 1982). Each block has its own specific geological history (Dalziel 1992). These crustal blocks are separated by fault systems, marked by deep ice-filled trenches.

3 Seismic Study

The seismic dataset for Antarctica comprised results from the analysis of teleseismic receiver functions, seismic reflection, and refraction data (Molinari and Morelli 2011) that were used to compile the ANTMoho model by Baranov and Morelli (2013). Moreover, we included results from processing the POLENET-ANET receiver functions that were used to determine the crustal thickness of West Antarctica by Chaput et al. (2014). A geographical distribution of seismic data is shown in Fig. 3.

3.1 Seismic Moho Model

We used data from 226 seismic stations and profiles to compile a new seismic Moho model for the Antarctic continent by applying a processing strategy similar to that used for the construction of recent continental-scale crustal models, for instance, by Grad et al. (2009), Baranov (2010), Lloyd et al. (2010), and Molinari and Morelli (2011). For this purpose, we

Journal : Small 10712 | Dispatch : 11-8-2017 | Pages : 34
Article No. : 9423 | ☐ LE | ☐ TYPESET
MS Code : GEOP-D-17-00046 | ☑ CP | ☑ DISK

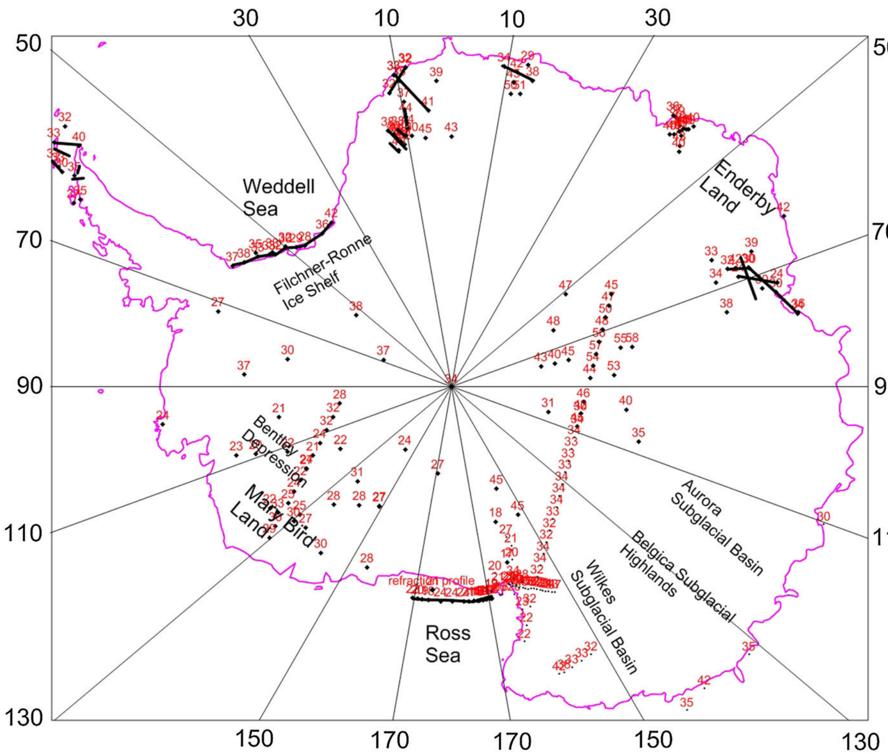

Fig. 3 Geographical distribution of seismic data in Antarctica

first inspected the quality of seismic data and then used them together with the BEDMAP2 subglacial bedrock relief to generate the Moho contours by applying a standard kriging technique with a linear variogram, while setting a scale factor equal to one. The linear variogram was intended for finding a local vicinity of the observed point and for weighting the observed points used in the function interpolation at a given grid point. The idea behind this geostatistical method is to reproduce trends that were estimated from combining the seismic data and the subglacial bedrock relief. Moreover, we set kriging parameters so that the interpolation area extended from the South Pole to the parallel 60 arc-deg of the southern latitude, with the 1 $\times$ 1 arc-deg equiangular geographical grid and no anisotropy. The resulting Moho grid was then limited by the Antarctic coastline (except for some small offshore areas). The seismic Moho model for the Antarctic continent is presented in Fig. 4 (for statistics see Table 4).

The new seismic model shows significant Moho depth variations. The average Moho depth under the Antarctic continent of 34.1 km closely agrees with a typical continental crustal thickness of about 34–35 km (according to global Moho models, e.g., CRUST1.0). The minimum Moho depth is detected in West Antarctica under the Ross Sea Ice Shelf (1–24 km) and Bentley depression (20–22 km). The maximum Moho deepening was detected under the Gamburtsev Subglacial Mountains (56–58 km) and Dronning Maud Land (48–50 km). Except for the Antarctic Peninsula (34–38 km) and Ellsworth Mountains (32–36 km), West Antarctica is characterized by a thin continental crust. Broad

Journal : Small 10712 | Dispatch : 11-8-2017 | Pages : 34
Article No. : 9423 | ☐ LE | ☐ TYPESET
MS Code : GEOP-D-17-00046 | ☑ CP | ☑ DISK

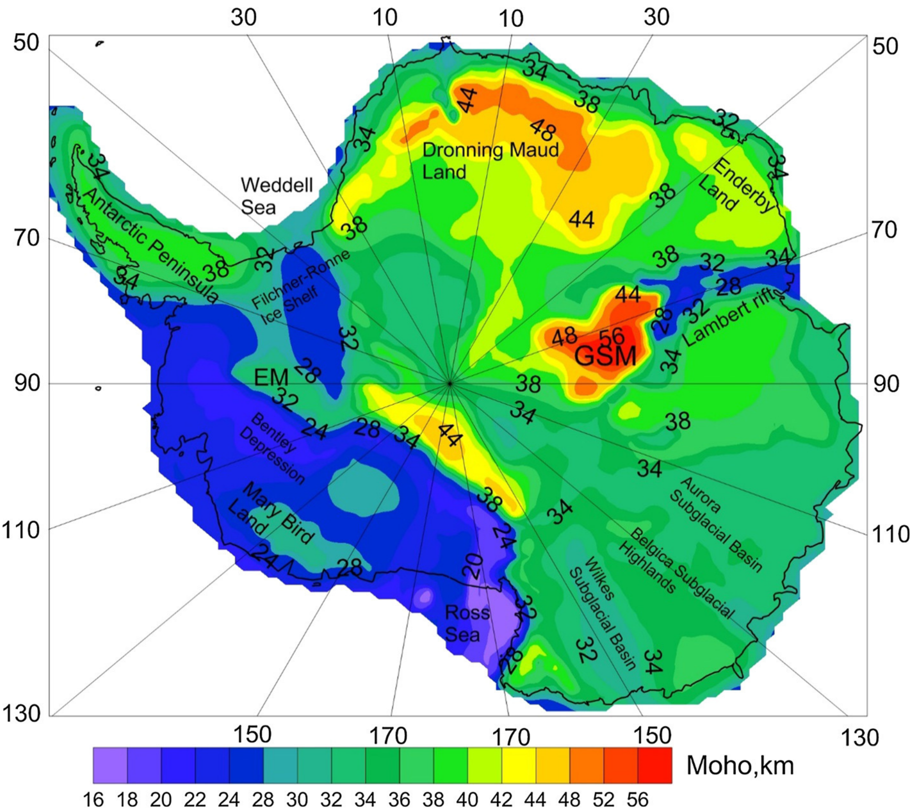

Fig. 4 Seismic Moho model for Antarctica. Used abbreviation: GSM—Gamburtsev Subglacial Mountains and EM—Ellsworth Mountains. Note that a *green color scale* indicates a typical continental crust with a Moho depth 28–40 km

regions with a normal or slightly shallow Moho are in East Antarctica, particularly a rift between western and central parts of Dronning Maud Land (30–34 km), Enderby Land (38–42 km), Lambert Rift (24–28 km), the South Pole region (32–36 km), Prince Charles Mountains (34–40 km), Princess Elizabeth Land (36–40 km), Aurora Subglacial Basin (30–34 km), Belgica Subglacial Highlands (34–36 km), and Wilkes Subglacial Basin (30–34 km). The Transantarctic Mountains mostly have a normal Moho (34–38 km) except for its central part (40–46 km).

3.1.1 *Comparison of Seismic Moho Models*

A regional comparison of our result with the global seismic crustal model CRUST2.0 (Bassin et al. 2000) and its more recent version CRUST1.0 (Laske et al. 2013) revealed significant differences (see Fig. 5a, b). In addition, we also compared our result with the regional seismic model ANTMoho (Baranov and Morelli 2013). Also in this case, we can see large localized differences (see Fig. 5c).

Journal : Small 10712 Dispatch : 11-8-2017 Pages : 34
Article No. : 9423 □ LE □ TYPESET
MS Code : GEOP-D-17-00046 ☑ CP ☑ DISK

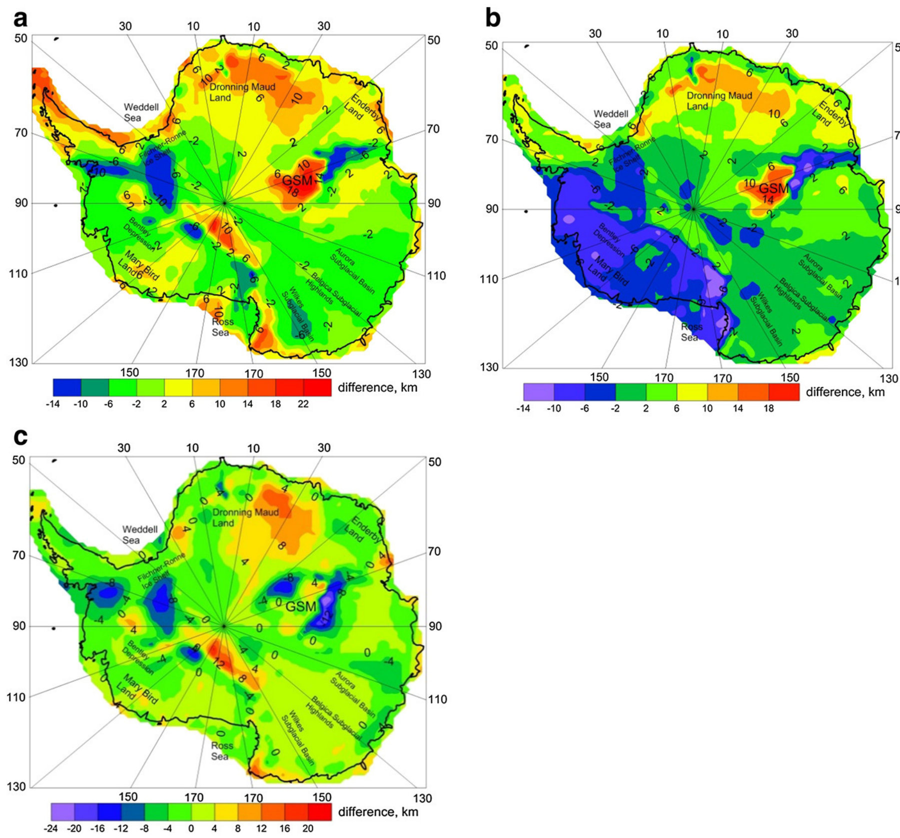

Fig. 5 Moho depth differences between our seismic model and **a** CRUST2.0, **b** CRUST1.0, and **c** ANTMoho

3.2 Seismic Sediment Model

Large parts of Antarctica are formed by subglacial sedimentary basins (Studinger et al. 2003; Bamber et al. 2006). However, throughout most of the Antarctic continent, the subglacial sediment structure is unknown. Since the distribution and character of subglacial sedimentary basins is one of the key constraints dictating basal ice dynamics (Blankenship et al. 1986; Alley et al. 1987), existing sediment thickness estimates have mainly been concentrated around regions of ice streaming in both East and West Antarctica, where the presence of sediments modulates ice-flow velocities. Among these estimates, Bamber et al. (2006) find evidence of 3-km-thick sediment accumulations below ice streams in East Antarctica (Slessor Glacier). Bell et al. (1998) reported the sediment thickness 1.0–2.4 km below ice streams in West Antarctica, while Anandakrishnan et al. (1998) estimated that, approximately 100 km away at the onset of streaming ice, the sediment is only 400–600 m thick. Sediment thickness estimates in the deep interior of Antarctica are rare.

We applied a numerical scheme used for a Moho modeling (in Sect. 3.1) to estimate the sediment thickness from the seismic data and the BEDMAP2 subglacial bedrock relief. Since sediment deposits are rather thick in some parts of Antarctica while the seismic velocity changes rapidly with depth, we compiled the sediment thickness model using three

Journal : Small 10712 Dispatch : 11-8-2017 Pages : 34
Article No. : 9423 LE TYPESET
MS Code : GEOP-D-17-00046 CP DISK

individual stratigraphic layers according to CRUST1.0. The upper sediment layer included all sedimentary basins with a thickness less than 2 km. For sedimentary basins of which thickness exceeds 2 km, we used this layer to describe a sediment density distribution down to 2 km. Below 2 km, we applied the middle sediment layer to describe sediment deposits down to the depth of 7 km and additional lower layer for sedimentary basins of which thickness exceeds 7 km. According to the empirical model between the P-wave velocity and the density (Brocher 2005), the sediment density in Antarctica varies from 2150 to 2500 kg m^{-3}. The thickness and P-wave velocities of sediment layers are summarized in Table 1. The seismic model of the total sediment thickness for Antarctica is shown in Fig. 6.

The sedimentary basins in Antarctica have different properties as well as origin. In West Antarctica, most of large sedimentary basins are associated with the extensional tectonism of that region. In the Ross Sea regions, the largest sedimentary deposits are accumulated along the Victoria, Central, and Eastern basins with the sediment thickness up to about 7 km according to the seismic profile ACRUP (Trey et al. 1999). The sedimentary basins attributed to the continental crustal extension were formed also in Weddell Sea Embayment, with the largest sedimentary basin under Filchner-Ronne Ice Shelf. According to results of seismic surveys presented by Huebscher et al. (1996) and Leitchenkov and Kudryavtzev (1997), the sediment thickness there varies from 2 to 14 km. Such large sediment accumulations in that region were also confirmed from the magnetic study conducted by Golynsky and Aleshkova (1997). According to the P-wave velocity diagram for WAIS station (Chaput et al. 2014), the thickness of sedimentary deposits in Bentley depression is about 4 km. Between Bentley depression and Ross Ice Shelf, the sediment thickness changes from 1 km (Rooney et al. 1987) to 2 km (Munson and Bentley 1992). Near the coast (Pine Island Glacier), the sediment thickness varies up to 2 km (Smith et al. 2013). Compared to West Antarctica, sedimentary basins in East Antarctica are much smaller. The sediment thickness in Lambert Rift is about 2–6 km (cf. Kolmakov et al.

Table 1 Thickness and velocities of sediment layers

Region	Thickness (km)				Vp (km s^{-1})		
	Total	Upper	Middle	Lower	Upper	Middle	Lower
Lambert Rift, Prince Charles Mountains, Princes Elizabeth Land (Kolmakov et al. 1975; Fedorov et al. 1982; Stagg et al. 2004)	0–6	0–2	0–4	0	3.4–3.5	3.6–3.7	–
Vostok Basin (Filina et al. 2008; Isanina et al. 2009)	0–4	0–2	0–2	0	3.8	4.7	–
Wilkes Subglacial Basin (Frederick et al. 2016)	0–1	0–1	0	0	3.4	–	–
Aurora Basin and Adventure Trough	0–1	0–1	0	0	3.2	–	–
Ross Sea (Trey et al. 1999)	1–7	1–2	0–5	0	3.2–3.4	4.1–4.4	–
Bentley depression (Chaput et al. 2014)	2–5	2	0–3	0	3.4	3.9–4.0	–
Filchner Ice Shelf (Huebscher et al. 1996; Leitchenkov and Kudryavtzev 1997)	2–15	2	0–5	0–7	2.7–3.0	3.7–3.9	4.8

Journal : Small 10712 Dispatch : 11-8-2017 Pages : 34
Article No. : 9423 ☐ LE ☐ TYPESET
MS Code : GEOP-D-17-00046 ☑ CP ☑ DISK

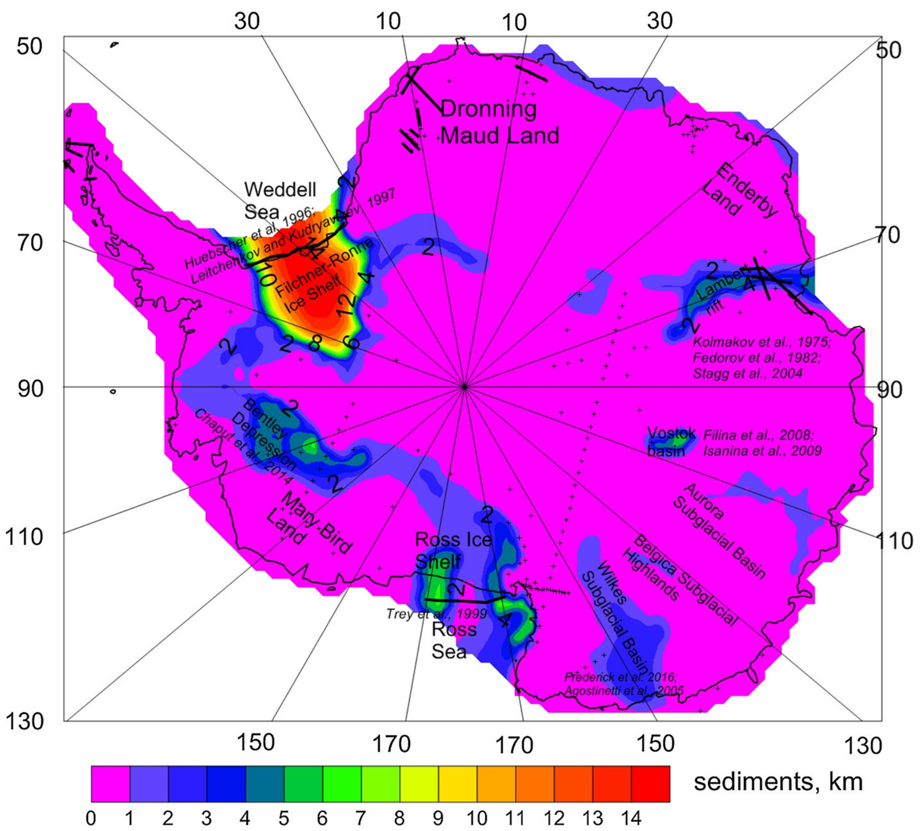

Fig. 6 Seismic model of the total sediment thickness for Antarctica, including used seismic data sources

1975; Mishra et al. 1999; Stagg et al. 2004). Another thick sediment deposits were detected in Vostok Basin, being the largest subglacial lake in East Antarctica, with a positive subglacial relief along the coast and the bedrock relief 1 km below sea level in its central part. According to geophysical data (Filina et al. 2008; Isanina et al. 2009), the sediment thickness there is about 2–4 km. The sediment thickness in Wilkes Subglacial Basin reaches 1 km (Frederick et al. 2016; Agostinetti et al. 2005). From the subglacial relief, we suggest that the sediment thickness in Aurora Basin and Adventure Trough is about 1 km (see Fig. 6).

3.2.1 *Comparison of Seismic Sediment Models*

Our results revealed large inconsistencies with the CRUST1.0 sediment thickness data in Antarctica (see Fig. 7). According to Laske et al. (2013), the average sediment thickness in the Antarctic continent is 0.6 km with maxima up to 5 km, while our result (Fig. 6) indicates that the average sediment thickness is 0.9 km with maxima up to 15 km under Filchner-Ronne Ice Shelf.

Journal : Small 10712 Dispatch : 11-8-2017 Pages : 34
Article No. : 9423 LE TYPESET
MS Code : GEOP-D-17-00046 CP DISK

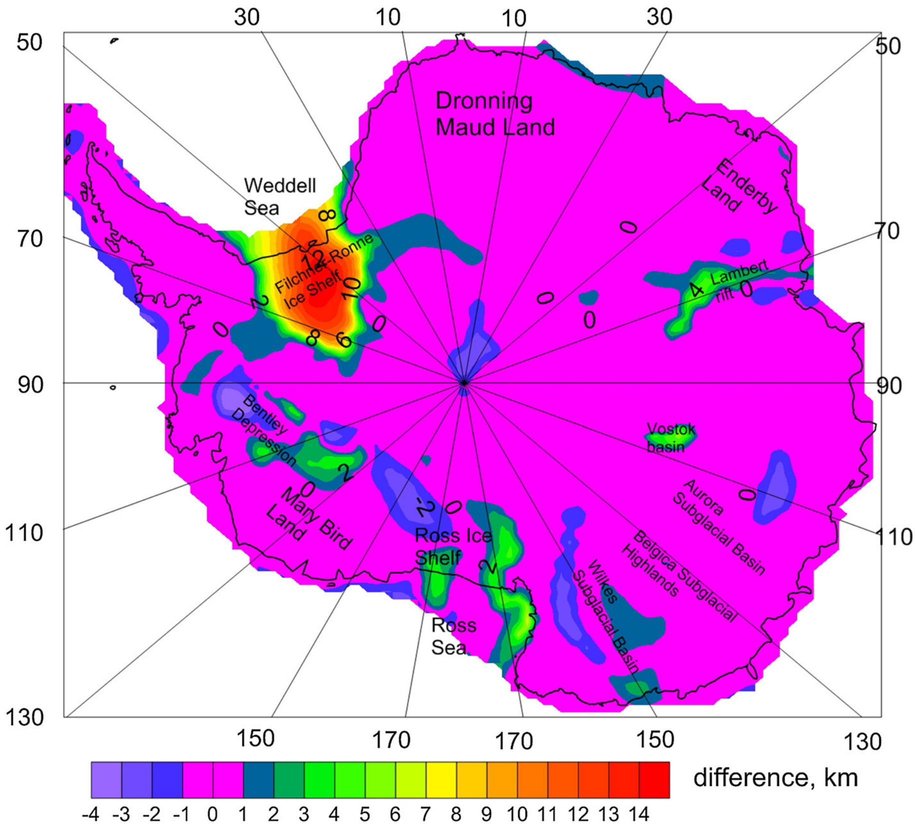

Fig. 7 Total sediment thickness differences between our and CRUST1.0 models

3.3 Seismic Consolidated Crustal Model

The depth down to the consolidated (crystalline) basement and the Moho interface are among parameters most reliably determined from seismic data. Seismic data can also be used to construct a more detailed model of the consolidated crust. However, the situation with the detection of individual stratigraphic layers within the crystalline crust is more complicated than with the Moho depth estimation. This is because depending on a given level of detail and a particular purpose of the analysis, different methods might provide a rather different stratification even in the same region. Here we applied again a three-layer model of the consolidated crust in order to ensure the consistency with CRUST1.0. However, it is worth mentioning that not all seismic data used for a Moho recovery were suitable for a detailed modeling of the crustal structure as well as for seismic velocity estimates. To assure the quality, we processed data only from seismic profiles that are the most appropriate for a stratification of the crystalline crust. In this respect, the most representative map for particular layers of the consolidated crust with seismic velocities was compiled for Dronning Maud Land (Hungeling and Tyssen 1991; Kudryavtzev et al. 1991; Kogan 1971), Enderby Land (Kanao et al. 2011), Lambert Rift, Prince Charles Mountains, Princes Elizabeth Land (Kolmakov et al. 1975; Fedorov et al. 1982), Ross Sea

(Trey et al. 1999), Filchner-Ronne Ice Shelf (Huebscher et al. 1996; Leitchenkov and Kudryavtzev 1997), Antarctic Peninsula (Grad et al. 1993), and Marie Bird Land (Kalberg and Gohl 2014). In our study, we used these seismic profiles to construct a three-layer model of the consolidated crust by interpolating a relative thickness of individual consolidated crustal layers with respect to their total thickness, because the percentage ratio of the thicknesses of particular layers varies more smoothly than their absolute thicknesses. Hence, we first interpolated relative thicknesses of the upper and middle layers, and subsequently determined a thickness of the bottom layer as a supplement up to 100%. We then converted these results into absolute values by multiplying them with the total thickness of the consolidated crust at each location. In regions where information about the crustal stratification is missing, we adopted values from CRUST1.0. In this way, we constructed a regional model of the consolidated crust, comprising information about the thickness and velocity of each layer. According to the empirical model between the P-wave velocity and the density (Brocher 2005), the density in Antarctica varies from 2530 to 2780 kg m^{-3} (within the upper consolidated crustal layer), from 2673 to 2860 kg m^{-3} (within the middle layer), and from 2740 up to 3120 kg m^{-3} (within the lower layer). The thickness and P-wave velocities of consolidated crust layers are summarized in Table 2.

To better illustrate tectonic features of the Antarctic continent, we show the total thickness of the consolidated crust (i.e., the crustal thickness without the glacial and sediment covers) in Fig. 8. The map revealed a complex crustal structure. Except for the Antarctic Peninsula (30–38 km), Marie Byrd Land (26–30 km), and Ellsworth Mountains (32–34 km), a thinned crust is found throughout whole West Antarctica, with a different thickness of the consolidated crust under Filchner-Ronne Ice Shelf (12–20 km), Ross Ice Shelf (10–22 km), and Bentley depression (16–20 km). We could also recognize more clearly (than in the seismic Moho map in Fig. 4) a variable crustal structure under the Ross Sea with thin crustal sections of the Victoria Land (including Central Basin) and Eastern Basin, which are separated by a thicker crust under the Central High. Broad regions of the extended crust in East Antarctica are located in Wilkes Subglacial Basin (26–30 km), Lambert Rift (18–24 km), Vostok Basin (24–28 km), and Aurora Subglacial Basin (28–30 km). A thin consolidated crust under the Lambert Trench confirmed a potential boundary between three blocks (Indo-Antarctica, the central East Antarctic Craton and Australia) that formed East Gondwana (Reading 2006). A thickened crust in East Antarctica was found under the Gamburtsev Subglacial Mountains and Dronning Maud Land. The largest thickness under the Gamburtsev Subglacial Mountains (56–58 km) indicates a presence of deep orogenic roots. In Dronning Maud Land, a thick consolidated crust of Wohlthat Massif (48–50 km) and Kottas Mountains (48–50 km) is separated by a relatively thin crust along Jutulstraumen Rift that represents a tectonic margin between the Grunehogna cratonic fragment and the late Neoproterozoic to Cambrian East African Antarctic Orogen (Marschall et al. 2013; Mieth and Jokat 2014; Jacobs et al. 2015). Other regions of East Antarctica have a normal continental crust, with slightly different crustal thickness under Enderby Land (36–40 km), Prince Charles Mountains (34–40 km), Princess Elizabeth Land (34–38 km), Belgica Subglacial Highlands (30–34 km), and the area of South Pole (30–36 km). The Transantarctic Mountains have a normal continental crust (34–38 km), except for its central part with a thickened crust (40–46 km).

Journal : Small 10712 | Dispatch : 11-8-2017 | Pages : 34
Article No. : 9423 | ☐ LE | ☐ TYPESET
MS Code : GEOP-D-17-00046 | ☑ CP | ☑ DISK

Table 2 Thickness and velocities of the consolidated crustal layers

Region	Thickness (km)				Vp (km s^{-1})		
	Total	Upper	Middle	Lower	Upper	Middle	Lower
Dronning Maud Land (Hungeling and Tyssen 1991; Kudryavtzev et al. 1991; Kogan 1971)	32–50	12–16	10–16	10–18	5.5–6.1	6.1–6.2	6.3–6.4
Enderby Land (Kanao et al. 2011)	36–40	16–20	10	10	6.1–6.3	6.5–6.6	6.8
Lambert Rift, Prince Charles Mountains, Princes Elizabeth Land (Kolmakov et al. 1975; Fedorov et al. 1982; Mishra et al. 1999; Stagg et al. 2004; Reading 2006)	18–24 34–40 34–38	6–8 10–12 10–12	6–8 10–12 16	6–8 14–16 8–10	5.4–5.6 5.7–5.9 5.4–5.6	5.8–5.9 5.8–5.9 5.8–6.0	6.1–6.2 6.1–6.2 6.2
Gamburtsev Mountains (Hansen et al. 2010)	44–58	–	–	–	–	–	–
Vostok Basin (Filina et al. 2008; Isanina et al. 2009)	24–28	–	–	–	–	–	–
Aurora Basin and Adventure Trough (An et al. 2015)	28–30	–	–	–	–	–	–
Belgica Highlands (An et al. 2015; Reading 2004)	30–34	–	–	–	–	–	–
Wilkes Subglacial Basin (Agostinetti et al. 2005; Bannister et al. 2003; Lawrence et al. 2006; Reading 2004)	26–30	–	–	–	–	–	–
Transantarctic Mountains (Lawrence et al. 2006)	34–46	–	–	–	–	–	–
Ross Sea (Bannister et al. 2003; Behrendt et al. 1991; Lawrence et al. 2006; Trey et al 1999)	10–22	2–7	3–5	5–10	5.6–5.9	6.1–6.4	6.7–7.3
Bentley depression (Winberry and Anandakrishnan 2004; Chaput et al. 2014)	16–20	–	–	–	–	–	–
Marie Byrd Land (Chaput et al. 2014; Kalberg and Gohl 2014)	26–30	6–10	8	12	5.5	6.0–6.5	6.5–7.5
Antarctic Peninsula (Grad et al. 1993)	30–38	8–10	6–10	16–18	5.6	6.2	6.6
Filchner-Ronne Ice Shelf (Huebscher et al. 1996; Leitchenkov and Kudryavtzev 1997)	12–20	3–5	3–5	6–10	5.0–5.5	6.5	7.1–7.4

4 Gravimetric Moho Model

We used the gravity, ice thickness, and crustal structure models to determine the Moho depth. This involved the use of gravity data over a broader area covering marginal seas and parts of the Southern Ocean in order to study the offshore extension of the Antarctic continental crust. The gravimetric Moho recovery was realized in two steps. Firstly, we

Journal : Small 10712 | Dispatch : 11-8-2017 | Pages : 34
Article No. : 9423 | ☐ LE | ☐ TYPESET
MS Code : GEOP-D-17-00046 | ☑ CP | ☑ DISK

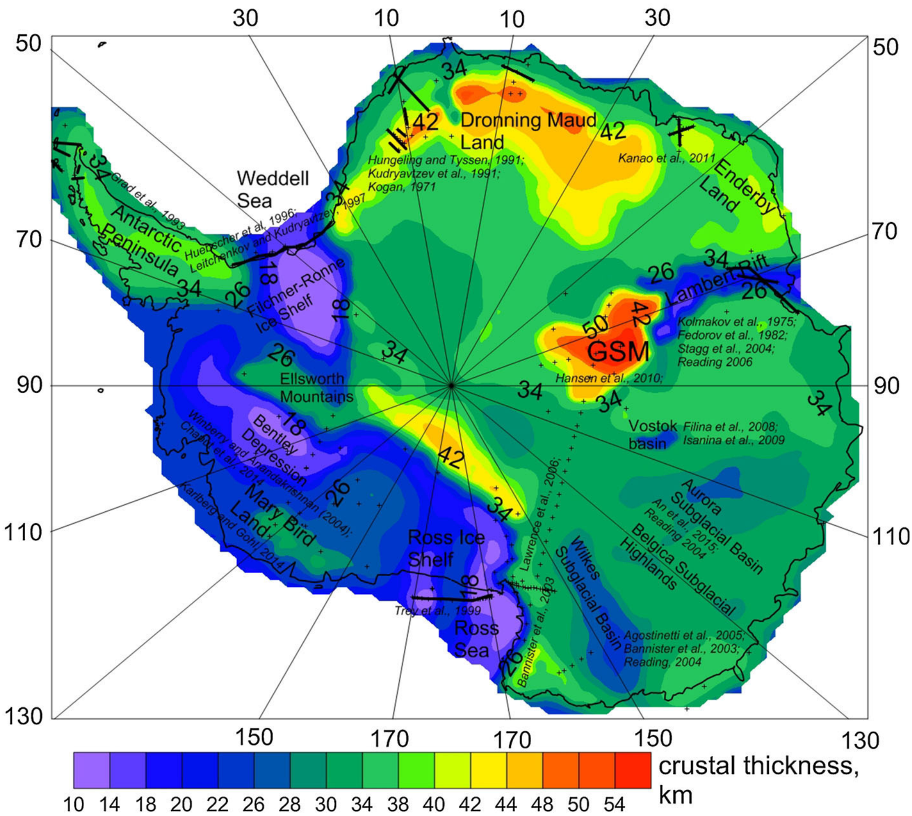

Fig. 8 Seismic model of the consolidated crust thickness for Antarctica, including used seismic data sources

applied the gravimetric forward modeling to compute the isostatic gravity data which were then used to determine the Moho depth by solving Vening Meinesz-Moritz's inverse problem of isostasy.

4.1 Gravimetric Forward Modeling

The gravimetric forward modeling was applied to compute the Bouguer and consequently isostatic gravity data.

4.1.1 Bouguer Gravity Data

We applied the topographic g^{T} and stripping gravity corrections due to density contrasts of the ocean (i.e., bathymetry) g^{B}, ice g^{I}, and sediments g^{S} to the (free-air) gravity disturbances δg in order to account for significant contributions of a rough subglacial relief, bathymetry (offshore), continental glaciers, sedimentary basins (inland), and marine sediments (offshore). The computation was performed according to the following scheme (Tenzer et al. 2009)

Journal : Small 10712 | Dispatch : 11-8-2017 | Pages : 34
Article No. : 9423 | ☐ LE | ☐ TYPESET
MS Code : GEOP-D-17-00046 | ☑ CP | ☑ DISK

$$\delta g^{\mathrm{cs}} = \delta g - g^{\mathrm{T}} + g^{\mathrm{B}} + g^{\mathrm{I}} + g^{\mathrm{S}}, \tag{1}$$

where δg^{cs} denotes the refined (Bouguer) gravity disturbance. Tenzer et al. (2015) demonstrated that the application of these gravity corrections yields the refined (Bouguer) gravity data that have a high spatial correlation with the Moho geometry. However, these gravity data still comprise the gravitational signal of (unmodeled) mantle density heterogeneities as well as errors due to crustal model uncertainties. The (long-wavelength) gravitational signature of the mantle can be removed either by applying spectral filtering techniques (Bagherbandi and Sjöberg 2012; see also Eckhardt 1983; Bowin et al. 1986) or by combining the gravity and seismic data. We applied the later method.

The (free-air) gravity disturbances δg in Eq. (1) were computed from the disturbing potential coefficients $T_{n,m}$ as follows (e.g., Heiskanen and Moritz 1967)

$$\delta g(r,\Omega) = \frac{\mathrm{GM}}{R^2} \sum_{n=0}^{\bar{n}} \sum_{m=-n}^{n} \left(\frac{R}{r}\right)^{n+2} (n+1)\, T_{n,m}\, Y_{n,m}(\Omega), \tag{2}$$

where $\mathrm{GM} = 3986005 \times 10^8\ \mathrm{m}^3\ \mathrm{s}^{-2}$ is the geocentric gravitational constant, $R = 6371 \times 10^3$ m is the Earth's mean radius, $Y_{n,m}$ are the surface spherical functions of degree n and order m, and $\bar{n}$ is the upper summation index of spherical harmonics. The 3-D position in Eq. (2) and thereafter is defined in the spherical coordinate system (r,Ω), where r is the radius, and $\Omega = (\phi, \lambda)$ is the spherical direction with the spherical latitude ϕ and longitude λ.

The gravity corrections in Eq. (1) were computed using the following generalized expression (Tenzer et al. 2012a, b, 2015)

$$g(r,\Omega) = \frac{\mathrm{GM}}{R^2} \sum_{n=0}^{\bar{n}} \sum_{m=-n}^{n} \left(\frac{R}{r}\right)^{n+2} (n+1) V_{n,m}\, Y_{n,m}(\Omega). \tag{3}$$

The potential coefficients $V_{n,m}$ of each volumetric density layer are defined by

$$V_{n,m} = \frac{3}{2n+1} \frac{1}{\bar{\rho}^{\mathrm{Earth}}} \sum_{i=0}^{I} \left(Fl_{n,m}^{(i)} - Fu_{n,m}^{(i)} \right), \tag{4}$$

where $\bar{\rho}^{\mathrm{Earth}} = 5500\ \mathrm{kg\ m}^{-3}$ is the Earth's mean density, and the coefficients $\{Fl_{n,m}^{(i)}, Fu_{n,m}^{(i)} : i = 0, 1, \ldots, I\}$ read

$$\mathrm{Fl}_{n,m}^{(i)} = \sum_{k=0}^{n+2} \binom{n+2}{k} \frac{(-1)^k}{k+1+i} \frac{L_{n,m}^{(k+1+i)}}{R^{k+1}}, \quad \mathrm{Fu}_{n,m}^{(i)} = \sum_{k=0}^{n+2} \binom{n+2}{k} \frac{(-1)^k}{k+1+i} \frac{U_{n,m}^{(k+1+i)}}{R^{k+1}}. \tag{5}$$

The coefficients $\{L_{n,m}^{(k+1+i)}, U_{n,m}^{(k+1+i)} : k = 0, 1, \ldots; i = 1, 2, \ldots, I\}$ in Eq. (5) describe the geometry and density (or density contrast) distribution within a particular volumetric density layer.

 We computed the gravity disturbances from the GOCO05S coefficients (corrected for the GRS80 normal gravity parameters; Moritz 2000) complete with the spherical harmonic degree of 180 (Eq. 2) and used the same spectral resolution to compute the gravity corrections (Eqs. 3–5). The topographic and bathymetric stripping gravity corrections were computed from the ETOPO1.0 data. The average upper continental crustal density of 2670 kg m^{-3} (Hinze 2003) was adopted for the topographic and reference crustal density. The bathymetric stripping gravity correction was evaluated for a depth-dependent seawater

Journal : Small 10712 Dispatch : 11-8-2017 Pages : 34
Article No. : 9423 LE TYPESET
MS Code : GEOP-D-17-00046 CP DISK

density model (Gladkikh and Tenzer 2011; see also Tenzer et al. 2011, 2012c). We used the BEDMAP2 data to compute the ice stripping gravity correction (see Tenzer et al. 2015) for the glacial density of 917 kg m^{-3} (Cutnell and Kenneth 1995). The sediment stripping gravity correction was evaluated using the CRUST1.0 sediment data (for continental sedimentary basins outside of Antarctica), a new seismic sediment model for Antarctica (Fig. 7), and a marine sediment density model (Tenzer and Gladkikh 2014; Chen et al. 2014). The regional maps of the free-air and refined Bouguer gravity disturbances, computed on a 1 × 1 arc-deg surface grid, are presented in Fig. 9, and their statistical summaries are given in Table 3.

The (free-air) gravity disturbances in Antarctica vary mostly within ±80 mGal, with gravity highs over the Antarctic Peninsula and large parts of East Antarctica and gravity lows mainly over the West Antarctic Rift System and the Transantarctic Mountains (Fig. 9a). As seen in the regional map of the refined Bouguer gravity disturbances in Fig. 9b, the application of the topographic and stripping gravity corrections substantially modified the gravity field in Antarctica. The most pronounced feature in the gravity pattern is the contrast between the continental and oceanic lithospheric structure along continental

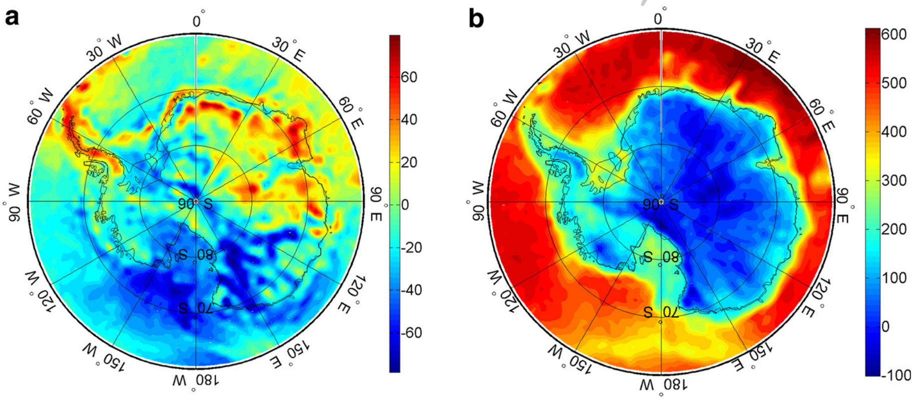

Fig. 9 Regional gravity maps (mGal): **a** GOCO05S gravity disturbances and **b** refined Bouguer gravity disturbances

Table 3 Statistics of the (stepwise) corrected gravity disturbances: the GOCO05S gravity disturbances δg (Fig. 9a), the topography-corrected gravity disturbances δg^{T}, the topography-corrected and bathymetry-stripped gravity disturbances δg^{TB}, the topography-corrected and bathymetry- and ice-stripped gravity disturbances δg^{TBI}, the refined Bouguer gravity disturbances δg^{cs} (Fig. 9b), and the isostatic gravity disturbances δg^{i} (Fig. 10b)

Gravity disturbances	Min (mGal)	Max (mGal)	Mean (mGal)
δg	−79	85	−13
δg^{T}	−487	43	−199
δg^{TB}	−317	562	74
δg^{TBI}	−122	569	182
δg^{cs}	−101	637	220
δg^{i}	−804	506	−132

Journal : Small 10712 Dispatch : 11-8-2017 Pages : 34
Article No. : 9423 ☐ LE ☐ TYPESET
MS Code : GEOP-D-17-00046 ☑ CP ☑ DISK

margins. Gravity highs are over the deep oceans and gravity lows are distributed throughout the central part of East Antarctica and over the Transantarctic Mountains.

4.1.2 *Isostatic Gravity Data*

The isostatic gravity disturbances δg^{i} were obtained from the refined Bouguer gravity disturbances δg^{cs} after applying the compensation attraction g^{c} (Moritz 1990), so that (cf. Tenzer and Bagherbandi 2012a, b)

$$\delta g^{\mathrm{i}} = \delta g^{\mathrm{cs}} + g^{\mathrm{c}}. \tag{6}$$

It is worth mentioning here that we computed the isostatic gravity disturbances instead of more commonly used isostatic gravity anomalies for geophysical interpretations. These aspects were discussed by Sjöberg (2013) and Tenzer et al. (2016), and numerically investigated by Tenzer and Bagherbandi (2012a, b).The compensation attraction g^{c} was computed from (Sjöberg 2009)

$$g^{c}(r,\Omega) \approx -4\pi G \Delta\rho^{c/m} D, \tag{7}$$

where $G = 6.674 \times 10^{-11}\ \mathrm{m^3\ kg^{-1}\ s^{-2}}$ is the Newton's gravitational constant, $\Delta\rho^{c/m}$ is the Moho density contrast, and the values of the Moho depth D were used from our new seismic model (Sect. 3.1).

The compensation attraction is everywhere negative (Fig. 10a), while the resulting isostatic gravity disturbances are typically positive offshore and negative inland with gravity lows over the Gamburtsev Subglacial Mountains (Fig. 10b).

4.2 Moho Inversion

Vening Meinesz-Moritz's inverse problem of isostasy is defined in the following generic form (Sjöberg 2013)

$$-GR\Delta\rho^{c/m} \iint_{\Phi} K(\psi, s)\,\mathrm{d}\Omega' = \delta g^{\mathrm{i}}(r,\Omega). \tag{8}$$

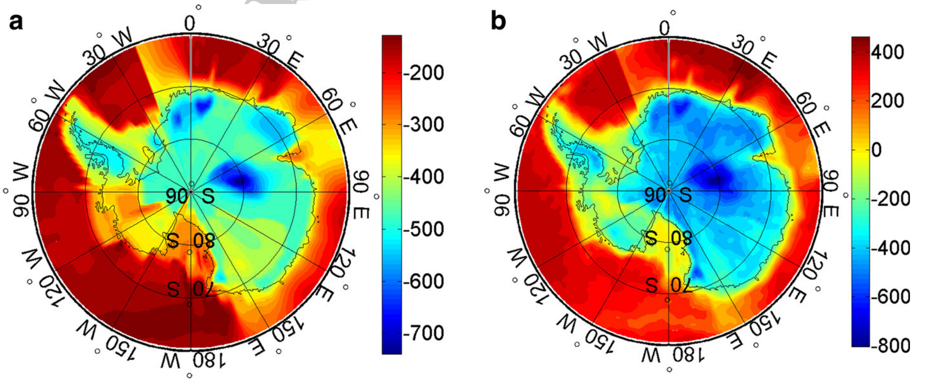

Fig. 10 Regional gravity maps of: **a** compensation attraction and **b** isostatic gravity disturbances (mGal)

Journal : Small 10712 | Dispatch : 11-8-2017 | Pages : 34
Article No. : 9423 | ☐ LE | ☐ TYPESET
MS Code : GEOP-D-17-00046 | ☑ CP | ☑ DISK

The integral kernel K in Eq. (8) is a function of the spherical angle ψ, and the parameter $s = 1 - D/R$ is a function of the Moho depth D. Its spectral form reads (cf. Sjöberg 2013)

$$K(\psi, s) = \sum_{n=0}^{\infty} \frac{n+1}{n+3} \left(1 - s^{n+3}\right) P_n(t), \tag{9}$$

where the Legendre polynomials P_n are defined for the argument $t = \cos\psi$.

The expression in Eq. (8) is (nonlinear) Fredholm's integral equation of the first kind. Its direct solution (up to a second-order term) was derived by Sjöberg (2009) in the following form

$$D(\Omega) = D_1(\Omega) + \frac{D_1^2(\Omega)}{R} - \frac{1}{32\pi R} \iint_{\Phi} \frac{D_1^2(\Omega') - D_1^2(\Omega)}{\sin^3(\psi/2)} \mathrm{d}\Omega'. \tag{10}$$

The Moho term D_1 in Eq. (10) was computed from the isostatic gravity coefficients $\delta g^{\mathrm{i}}_{n,m}$ as follows

$$D_1\,(\Omega) \approx \frac{1}{4\pi G \Delta\rho^{c/m}} \sum_{n=0}^{\bar{n}} \left(2 - \frac{1}{n+1}\right) \sum_{m=-n}^{n} \delta g^{\mathrm{i}}_{n,m} Y_{n,m}(\Omega). \tag{11}$$

The singularity for $\psi \to 0$ in the third constituent on the right-hand side of Eq. (10) was solved by applying the surface integration over the inner zone (cf. Sjöberg 2009).

The gravimetric Moho model is shown in Fig. 11 (for statistics see Table 4). The Moho depth under oceans is typically less than 15 km, while it increases to about 25–30 km

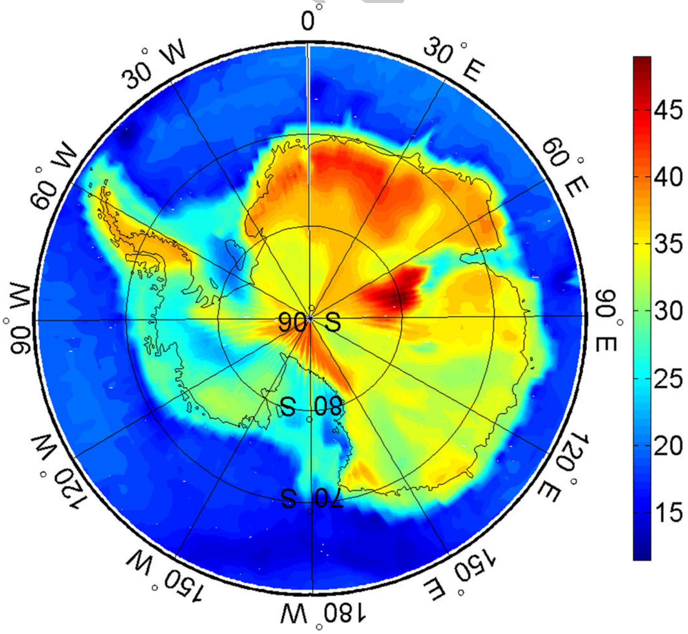

Fig. 11 Gravimetric Moho model (km) for Antarctica

Journal : Small 10712 Dispatch : 11-8-2017 Pages : 34
Article No. : 9423 LE TYPESET
MS Code : GEOP-D-17-00046 CP DISK

Table 4 Statistics of Antarctic Moho models

Moho model	Min (km)	Max (km)	Mean (km)
Seismic (inland)	16.5	58.2	34.1
Gravimetric	11.4	49.7	28.9
Combined	8.2	62.4	29.0
CRUST1.0	9.0	43.5	34.0

along continental margins. The maximum Moho deepening in Antarctica of 49.7 km is under Gamburtsev Subglacial Mountains.

5 Combined Moho Model

In order to reproduce the seismic model more realistically, we constrained the gravimetric solution by seismic data. For this purpose, we used the method of Bagherbandi and Sjöberg (2012) that was later applied, for instance, by Bagherbandi et al. (2013, 2015). The principle of this method is to compute the non-isostatic gravity correction in order to account for the differences between the gravimetric and seismic Moho models. The non-isostatic gravity correction is then applied to the isostatic gravity disturbances. The resulting isostatic gravity disturbances obtained after applying the non-isostatic correction were then used to compute the combined Moho model according to the VVM isostatic model (Eqs. 10 and 11). The result is shown in Fig. 12 (for statistics see Table 4).

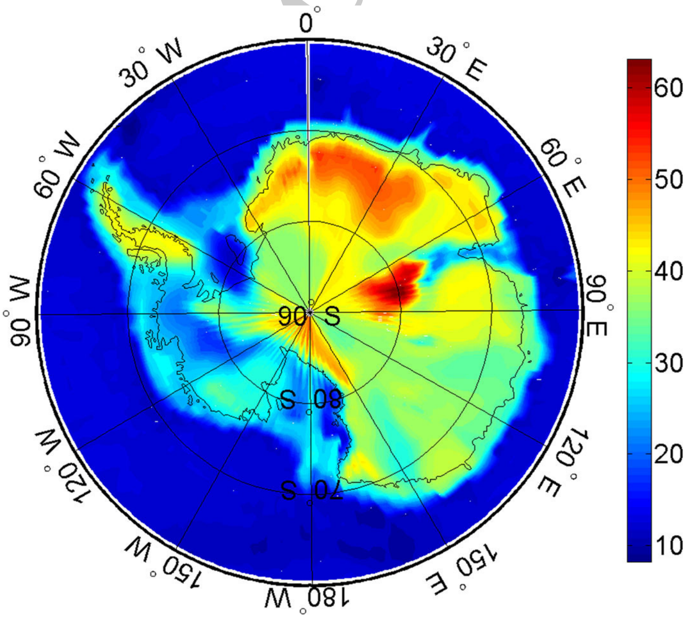

Fig. 12 Combined Moho model (km) for Antarctica

Journal : Small 10712 | Dispatch : 11-8-2017 | Pages : 34
Article No. : 9423 | ☐ LE | ☐ TYPESET
MS Code : GEOP-D-17-00046 | ✔ CP | ✔ DISK

6 Comparison of Results

The comparison of our gravimetric and seismic models revealed only a small systematic bias (of about 2 km), but large (regional-scale) differences mostly within ±10 km (see Fig. 13a, and statistics of difference in Table 5). As shown in Fig. 13a, the gravimetric Moho depth is systematically underestimated under Dronning Maud Land, the Gamburtsev Mountains, and the Antarctic Peninsula, while overestimating under Filchner-Ronne Ice Shelf and the Ross Sea as well as along continental rift zones of the Lambert and Bentley Trenches. As expected, the combination of gravity and seismic data improved the RMS fit of the combined model with the seismic one (Table 5), but the combined model systematically overestimates the Moho depth (Fig. 13b). Moreover, the differences between these two models typically increase with the Moho depth so that we could see relatively small differences under the oceanic crust, continental margins and continental rift zones, with increasing differences under the extended continental crust, and the maximum differences under orogens corresponding to a maximum Moho deepening. Under the Ross Sea, Filchner-Ronne Ice Shelf, the Lambert and Bentley Trenches, the differences between the combined and seismic models are typically less than 1 km. Elsewhere within the Antarctic continent, these differences increase to 2–4 km and reach maxima of 4.9 km under

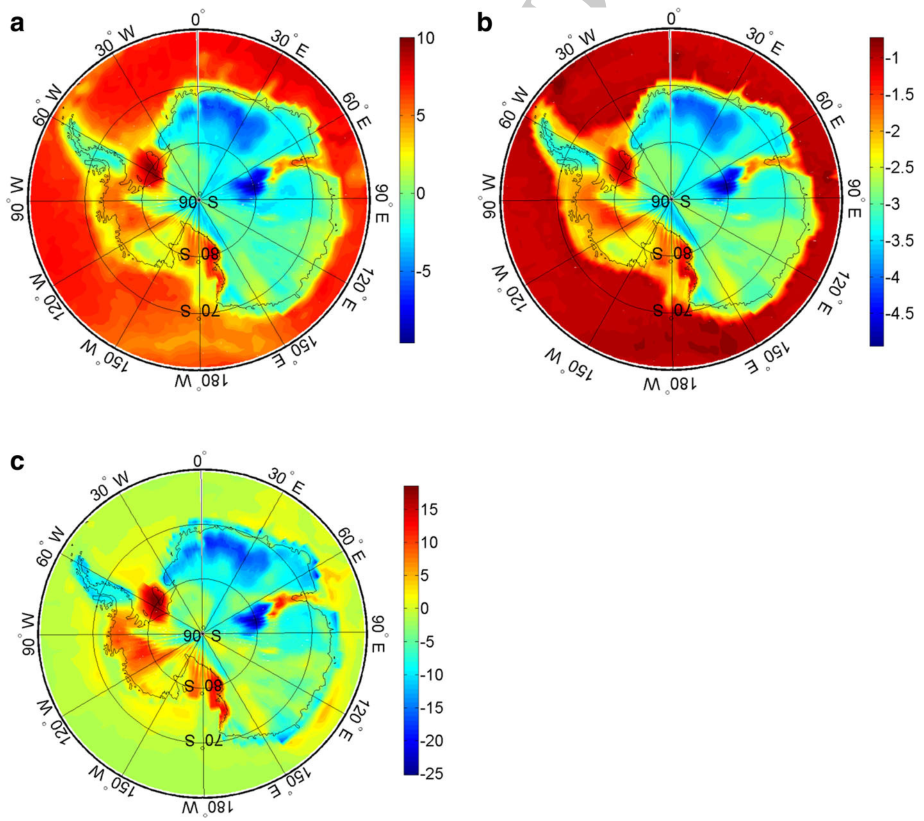

Fig. 13 Differences between the Moho models (km): **a** gravimetric–seismic, **b** seismic–combined, and **c** CRUST1.0–combined

Journal : Small 10712 Dispatch : 11-8-2017 Pages : 34
Article No. : 9423 LE TYPESET
MS Code : GEOP-D-17-00046 CP DISK

Table 5 Statistics of the Moho differences

Moho differences	Min (km)	Max (km)	Mean (km)	RMS (km)
Gravimetric–seismic	−9.5	10.4	2.1	4.4
Seismic–combined	−4.9	−0.6	−2.2	2.4
CRUST1.0–combined	−25.2	19.4	−1.8	5.8

Dronning Maud Land. In contrast to a relatively good agreement between the combined and seismic models, we could see significant misfit of the combined model with CRUST1.0, with the maximum differences locally exceeding even 20 km (Fig. 13c).

7 Moho Uncertainties

The accuracy of newly developed combined Moho model for Antarctica depends on several factors, mainly related to a quality of input gravity and seismic data as well as available information on the crustal structure (involving topographic, bathymetric, ice thickness, sediment, and consolidated crust data). Large errors in estimated values of the Moho depth from seismic data were reported in different parts of the world. Grad et al. (2009), for instance, demonstrated that the Moho depth uncertainties estimated using seismic data in Europe regionally exceed 10 km, with an average error of about 4 km. Even larger Moho depth uncertainties could be expected in Antarctica due to much lower and irregular seismic data coverage.

The best horizontal Moho resolution is typically inferred from reflection profiles (cf. Kanao et al. 2011), but such technique is expensive, and thus not widely used. The Moho detection from a two-way travel time might also be affected by a weak reflectivity. An intermediate spatial resolution could be obtained from a deep seismic sounding based on using refracted and wide-angle reflected waves. The uncertainties of detecting the Moho depth from the wide-angle reflection and refraction methods are typically about 1–2 km. Another technique, which became quite common during the last two decades, is based on inverting the P- or S-wave receiver functions (e.g., Zhu and Kanamori 2000; Hansen et al. 2009). An estimated uncertainty of this method is about 3 km. The intermediate-period surface waves are quite sensitive to the crustal thickness, but are not able to discriminate it from the mantle velocity structure, and thus cannot be inverted uniquely (cf. Danesi and Morelli 2001; Kobayashi and Zhao 2004; Ritzwoller et al. 2001). A wide station spacing and the absence of intraplate earthquakes in Antarctica do not generally allow inverting the short-period surface waves which have a better sensitivity to a shallower density structure. However, surface waves are useful for studying areas where other types of seismic data are not available (such as Antarctic interior).

To interpolate the Moho information over large parts of Antarctica where seismic data are missing, we used the gravity data and additional information about the crustal structure. The Moho depth uncertainties attributed to errors in gravity data are relatively small, because the accuracy of the latest global gravitational models of about ±10 mGal or better is expected globally at a resolution of about 100 km (cf. Pail et al. 2010, 2011a, b). However, larger errors in combined global gravitational models (including the GOCO05S) are expected inland of Antarctica due to the absence of gravity information. The most significant is the polar gravity data gap of the GOCE mission of about 6.5 arc-deg, which affects mainly the higher-degree spherical harmonics of the gravity field that are not

Journal : Small 10712 Dispatch : 11-8-2017 Pages : 34
Article No. : 9423 □ LE □ TYPESET
MS Code : GEOP-D-17-00046 ☑ CP ☑ DISK

observed accurately by the GRACE gravity mission. The polar gap problem of the GRACE mission is obviously less significant, because the GRACE orbit has the inclination of about 89.0 arc-deg. Further improvement in the gravity information is expected in the near future due to the availability of new airborne gravity data over Antarctica (see, e.g., Forsberg et al. 2011). Relatively small errors due to topographic/bathymetric model uncertainties are expected, because these models are also provided with a relatively high accuracy and resolution. Rodriguez et al. (2006) discussed in detail accuracy characteristics of the Shuttle Radar Topography Mission (SRTM) elevations. Comparisons with ground control points, whose elevations were determined independently using kinematic GPS positioning, indicated that the 90% absolute error of the SRTM elevations is typically within ± 10 m, depending on a relief. Since large parts of marine areas (particularly with a permanent sea ice) have not yet been covered by the sounding reflection surveys, the marine gravity data are primarily used to determine bathymetric depths. Although the estimation of errors of the gravimetrically determined bathymetric depths is not simple, it could be expected that most of errors have the origin in uncertainties of the gravity-to-topography transfer function. Apart from these errors, the Moho uncertainties also depend on applied density models. For the computation of topographic gravity correction, we adopted a constant density of 2670 kg m^{-3}. This density value is often assumed for the upper continental crust and corresponds to a mean density of crystalline and granitic rocks. The density of granitic rocks ranges from 2500 to 2800 kg m^{-3}, with a mean value about 2670 kg m^{-3}. According to Hinze (2003), the crystalline rocks represent roughly 25% of the continental crust, while the remaining 75% is formed by sedimentary rocks consisting of about 65% of shale (2000–2700 kg m^{-3}), 20–25% sandstones (2000–2700 kg m^{-3}), and 10–15% carbonate rocks (2500–2900 kg m^{-3}). As evident from this variable geological composition, the approximation of the crustal density by a constant value could yield large Moho uncertainties (up to 10%). The Moho uncertainties attributed to the approximation of the seawater density distribution are, on the other hand, much smaller. Maximum errors of the depth-dependent seawater density model (applied to compute the bathymetric stripping gravity correction) are less than 0.6%, while the corresponding average error is only about 0.1% (cf. Tenzer et al. 2012a)

To account for a large glacial cover in Antarctica, we applied the ice stripping correction to gravity data. The Moho uncertainties due to ice density depend mostly on the accuracy of ice thickness data. Being constructed from data with a variable spatial resolution, the subglacial bedrock uncertainties vary across the continent. Lythe et al. (2001) reported errors typically 150–300 m, with maxima up to about 400 m in regions with rough subglacial bedrock topography. Moreover, parts of the BEDMAP2 data were derived directly from the gravity data (cf. Fretwell et al. 2013). Hence, the ice thickness information over these regions is influenced by gravity data uncertainties. In addition, the surface elevation model within the polar gap in satellite altimetry coverage may be in error by up to about 100 m. To assess the influence of subglacial bedrock uncertainties on the Moho depth, we assumed errors of ± 300 m and estimated the corresponding Moho depth changes. According to our estimates (not shown herein in detail), these uncertainties contribute less than 0.7 km on the Moho depth. Uncertainties due to adopting a constant density of the glacial ice (917 kg m^{-3}) mainly depend on a ratio of the firn ice layer and the consolidated glacial ice. Tenzer et al. (2010) estimated that a lower density of the firn ice than the glacial ice density can be accounted for by reducing a total ice thickness not more than 20–25 m. Compared to the total ice thickness and expected uncertainties in the subglacial bedrock topography, this value is negligible. The contribution of the sea ice density, which has large seasonal variations, was not taken into consideration.

Journal : Small 10712 Dispatch : 11-8-2017 Pages : 34
Article No. : 9423 □ LE □ TYPESET
MS Code : GEOP-D-17-00046 ✔ CP ✔ DISK

The largest Moho errors in the gravimetric solution are expected due to uncertainties of the CRUST1.0 sediment and consolidated crustal layers. Therefore, we used seismic data to improve this model in Antarctica. Our results (in Sect. 3) revealed large modifications in the sediment thickness. The gravity anomaly associated with sedimentary basins can be either positive or negative depending on the overall feature size and strength of the lithosphere during rifting and infill (Karner et al. 2005). Since we used fixed subglacial bedrock topography, the depth to geologic basement cannot be distinguished from the surface of sedimentary basins. Whereas a 400–600-m-thick sediment layer causes the Moho uncertainty of less than 0.5 km, the Moho uncertainty of about 1.5 km corresponds to a 3-km-thick layer, while 15-km-thick sediments (found under Filchner-Ronne Ice Shelf) could modify the Moho depth as much as 4 km. However, these values are probably overestimated, because large sediment deposits modify directly the Moho geometry so that a simple linear relation between the sediment and crustal thickness uncertainties is not realistic.

The Moho density contrast of 480 kg m^{-3} was adopted in our gravimetric inversion, rather than as the difference of the consolidated crust and upper mantle layers, to allow for an increase in the crustal density under confining pressures. The shear-wave velocity studies published by Ritzwoller et al. (2001) and Morelli and Danesi (2004) revealed that the mantle velocity is different in East and West Antarctica and changes with depth. The transition is particularly significant in amplitude and parallel to the Transantarctic Mountains at 80 km depth, and weaker at both shallower and deeper depths. In the uppermost mantle, Ritzwoller et al. (2001) predicted variability throughout Antarctica of no more than ±2% with respect to the 1-D velocity model AK135 (Kennett et al. 1995). Using the basic equations for the shear-wave velocity, we estimated that the Moho density contrast is everywhere within ±130 kg m^{-3} of the AK135 predicted upper mantle value of 2976 kg m^{-3}. Since a spatial distribution of the Moho velocity changes is poorly constrained by the current distribution of passive seismic arrays, we have not tried to simulate it in our model. Instead, we have centered our estimate on a reasonable value for the Moho density contrast and modeled the effect of the predicted variability as an uncertainty around our solution. We adopted a reasonable estimate for the Moho density contrast of 480 kg m^{-3} and suggested that a 130 kg m^{-3} envelope around this value is consistent with the work of Ritzwoller et al. (2001). This variability causes the Moho depth uncertainties within ±1.7 km.

8 Discussion

The seismic Moho model (Fig. 4) closely resembles the Antarctic geological structure, composed of a variety of tectonic features ranging from the Archean to Cenozoic. The most prominent feature is the contrast between East and West Antarctica. A relatively thick crust of East Antarctic Shield is separated by a thin crust of the continental rift zone from a more complex structure of West Antarctica that is composed by an assemblage of several tectonic blocks of different geological origin and composition.

The crustal thickness of West Antarctica is characterized by a shallow Moho under most of the West Antarctic Rift System, while a regional Moho deepening was detected under the Ellsworth Mountains, the Antarctic Peninsula, and Marie Bird Land. Under the Ellsworth Mountains, with the highest mountain peaks in Antarctica (2–3 km in average), the Moho depth reaches 32–34 km. The Moho relief in the Antarctic Peninsula, with the

Journal : Small 10712 Dispatch : 11-8-2017 Pages : 34
Article No. : 9423 LE TYPESET
MS Code : GEOP-D-17-00046 CP DISK

subglacial elevations reaching 2–3 km, indicates a possible absence of orogenic roots under these Antarctic Andes, with the Moho depth ranging from 34 km (near its margins) to about 38 km (inland). The Moho under Marie Bird Land deepens to 26–30 km, while the ice cover varies also significantly (0–2 km). This lithospheric structure is characterized by a topographic doming likely caused by a localized hot spot activity (Hole and LeMasurier 1994; Winberry and Anandakrishnan 2004).

The Moho depth under the West Antarctic Rift System is typically shallow with depths mostly within 16–32 km. More pronounced Moho irregularities are under the Ross Sea Ice Shelf (16–24 km) and the Filchner-Ronne Ice Shelf (26–30 km). In central part of the rift zone an additional distinctive feature is recognized under the Bentley Trench, with a deep subglacial relief (to about 2.5 km below sea level), thick ice fill (2–3 km), and the Moho depth 20–22 km. The West Antarctic Rift System is unique among continental rift systems in being associated with low intraplate deformation rates (Wilson et al. 2011), low seismicity (Winberry and Anandakrishnan 2003; Reading 2007), thin crust (Winberry and Anandakrishnan 2004), low viscosity of the mantle (Wiens et al. 2012), and localized high heat flow (Clow et al. 2012). Its geological evolution was associated with volcanism occurring since (at least) the Early Cenozoic. According to Behrendt et al. (1991), the main rifting phase occurred between 105 and 85 Myr, although the episodic extension continued into the Cenozoic. The extension within the rift system has left most of West Antarctica below sea level, except for Marie Byrd Land, Ellsworth Mountains, and parts of the Antarctic Peninsula. Some studies suggest that this represents remains of a continuously propagating rift that started during the Jurassic period when Africa separated from East Antarctica and proceeded clockwise to its present location in the Ross Sea Embayment and West Antarctica. Almost complete absence of recent seismic activity indicates that there is no any undergoing active extension of the rift zone (Cande et al. 2000), but the Holocene volcanism in the Ross Sea Embayment (Kiele et al. 1983; Blankenship et al. 1993; Behrendt et al. 1991) suggests a possible presence of active tectonism in that part of the rift zone.

Although seismic data over some parts of East Antarctica are still sparse, major geological and tectonic features (composed of cratons, shields, subglacial orogens, continental basins, and continental rifts) are clearly recognized in the Moho relief (Fig. 4) and even better manifested in the map of the total consolidated crust (Fig. 8). The Moho depth under East Antarctica varies from 23 to about 58 km, with its minima under the Lambert Trench and maxima under the Transantarctic Mountains, Dronning Maud Land, and Gamburtsev Subglacial Mountains. The Transantarctic Mountains have high subglacial elevations (2–3 km) and the Moho depth from 34 km (along its margins) to 46 km (in central part). The maximum Moho depth (44–58 km) in Antarctica was found under the Gamburtsev Subglacial Mountains, characterized by deep orogenic roots (possibly as much as 10–15 km relative to the surrounding Moho topography), high subglacial bedrock elevations (2–3 km), and large ice cover (1.4–2.0 km). Another significant Moho depending was detected under Dronning Maud Land. The Moho there deepens to 48–50 km and bedrock elevations reach 2–3 km with almost no ice. The Moho depth under Enderby Land is typically 38–42 km. The Moho under Mac. Robertson Land exhibited large variations with a substantial crust thinning along the Lambert Rift. The Moho depth there decreases to only 24–28 km, while a large ice cover (1.0–3.5 km) fills deep bedrock depression (1.5 km below sea level). The Moho relief in East Antarctica also resembles the subglacial bedrock relief across Aurora and Wilkes basins, separated by a slightly thicker crust of the Belgica Subglacial Highlands, but the Moho topography is rather smooth (mostly 30–34 km).

Journal : Small 10712 Dispatch : 11-8-2017 Pages : 34
Article No. : 9423 LE TYPESET
MS Code : GEOP-D-17-00046 CP DISK

The gravimetric model for Antarctica (Fig. 12), comprising also the Moho information under surrounding oceans, revealed the contrast between thin oceanic and thick continental crustal structures, marked by a Moho deepening under continental margins. The largest (offshore) continental crustal extension was detected on both sides of the West Antarctic Rift System between the Weddell Sea Embayment and the Ross Sea Embayment. The contrast between West and East Antarctica is clearly marked by a thin crust of continental rift zone. Another dramatic contrast is seen between the Gamburtsev Subglacial Mountains and Lambert Rift. Here Moho changes rapidly from 58 to only 24 km. In West Antarctica, the Moho regionally deepens under the Antarctic Peninsula, Marie Byrd Land, and partially also under the Ellsworth Mountains. In East Antarctica, the Moho deepens under Dronning Maud Land, the Transantarctic Mountains, and reaches a maximum depth under the Gamburtsev Subglacial Mountains.

Despite overall similarities between our gravimetric and seismic Moho models, some large regional differences between these two models exist (Fig. 13a). The gravimetric model could not reproduce realistically the Moho at some places, because detailed topographic features and lithospheric density heterogeneities are not fully isostatically compensated. Moreover, the isostatic mass balance depends on the loading and effective elastic thickness, rigidity, rheology of the lithosphere, and viscosity of the asthenosphere, and other geodynamic phenomena (such as plate tectonics, mantle convection, ice sheet dynamics) which are not described by the VMM compensation mechanism defined based on a thin plate lithospheric flexure model (Watts 2001). The gravimetric solution systematically underestimated the Moho depth under orogens, while overestimating under continental rift zones (Fig. 13a). A systematic bias between the gravimetric and seismic models might to some extent be also attributed to the (ongoing) glacial isostatic adjustment mainly in the Antarctic Peninsula, because the lithospheric and mantle relaxation due to variations in ice load takes place over timescales 10^5–10^7 years (Johnson et al. 2000).

The combination of the gravity and seismic data improved significantly the RMS fit of the resulting (combined) Moho model with the seismic one (Fig. 13b). The combined model also reproduced more closely most of major Moho features that were detected from seismic data. A very close agreement was attained particularly along continental margins and continental rift zones. The misfit between the combined and seismic model systematically increases with Moho depth and reaches maxima of 4.9 km under the Gamburtsev Subglacial Mountains.

9 Concluding Remarks

The Antarctic tectonic plate consisting of the continental lithosphere of significantly different age, origin, and geological composition is surrounded by the oceanic lithosphere formed along the mid-oceanic rift zones, while oceanic subductions are typically absent, except for the Antarctic tectonic margins with the South American, Scotia, and Shetland plates. Whereas the West Antarctic complex geological structure was formed mainly by the compressional tectonism, the extensional tectonism was a dominant force of forming the West Antarctic Rift System, comprising the continental rift and possibly also a hot spot location (under Marie Bird Land). Although most of East Antarctica is composed mainly by a stable ancient craton and shield, more detailed geological features include orogens, continental basins, and rifts. These major geological and tectonic features are clearly manifested in the Moho relief presented in this study. The Moho depth in Antarctica has

Journal : Small 10712 | Dispatch : 11-8-2017 | Pages : 34
Article No. : 9423 | ☐ LE | ☐ TYPESET
MS Code : GEOP-D-17-00046 | ☑ CP | ☑ DISK

been also modified by volcanism, sediment accumulation, and significant ice load variations, but these temporal variations were out of the scope of this study.

Our results showed that the oceanic crust surrounding Antarctica is typically less than 15 km. The Antarctic continental crustal extension, characterized by a significant Moho deepening under continental margins, is more pronounced along East Antarctic margin where Moho reaches depth typically 30 km or more. In contrast, the Moho under continental margins in West Antarctica is shallower and a thin continental crust (typically 20–30 km) further extends inland along the West Antarctic Rift System, with three distinctive locations under the Ross Sea, Weddell Sea, and the Bentley Trench. The Moho in West Antarctica deepens under Marie Bird Land, the Ellsworth Mountains, and in the Antarctic Peninsula where it reaches maximum depth about 38 km.

The Moho relief in East Antarctica is much more complex than that presented in previous studies. The most pronounced is the well-known Moho deepening under the Gamburtsev Subglacial Mountains. The seismic data analysis revealed that the maximum Moho depth there reaches 58.2 km (while the result from combining seismic and gravity data gave slightly larger value of 62.4 km). The Moho topography there indicates the presence of relatively deep and compact orogenic roots. Other small orogenic roots were detected under Kottas Mountains and Wohlthat Massif in Dronning Maud Land with Moho reaching 50 km. Another significant feature in East Antarctica was detected along the Lambert Trench, characterized by a thin extensional continental crust with the Moho depth only 24–28 km. The seismic data analysis revealed that a rather thick crust of the Transantarctic Mountains is separated from the rest of East Antarctica by a thinner crust that begins under the Wilkes Subglacial Basin and continues inland under the South Pole toward the Filchner-Ronne Ice Shelf. This Moho feature is almost parallel with the West Antarctic Rift System. Although the Moho under the Transantarctic Mountains deepens as much as 46 km, the presence of orogenic roots is still open for discussion. The seismic data analysis also exhibited some more detailed Moho features (seen also in the gravimetric result), showing that continental basins of Wilkes Subglacial Basin and Aurora Subglacial Basin are separated by a thicker crust of Belgica Subglacial Highlands.

Our seismic data analysis revealed a much more complex structure of continental sedimentary basins in Antarctica. A maximum sediment thickness up to about 15 km under Filchner-Ronne Ice Shelf differs significantly from the CRUST1.0 model, suggesting a maximum thickness there up to only 5 km. We also demonstrated a complex and inhomogeneous structure of the consolidated crust with an extremely thin continental crust (10–20 km) under Ross Sea and the Ronne Ice Shelf, while reaching maximum thickness of 56 km under the Gamburtsev Subglacial Mountains.

Acknowledgements The National Science Foundation of China (NSFC) is cordially acknowledged for a financial support by the research Grant No.: 41429401. We also acknowledge a financial support from the Russian Foundation for Basic Research under two research Grants: 16-55-12033 and 13-05-01123.

References

Adams RD (1971) Reflections from discontinuities beneath Antarctica. Bull Seismol Soc Am 5:1441–1451

Agostinetti P, Roselli P, Cattaneo M, Amato A (2005) Moho-depth and subglacial sedimentary layer thickness in the Wilkes Basin from Receiver Function Analysis. IASPEI. General Assembly, October 2.9, 2005, Chile, Abstracts Volume, pp 281–284

Airy GB (1885) On the computation of the effect of the attraction of mountain-masses, as disturbing the apparent astronomical latitude of stations in geodetic surveys. Philos Trans R Soc Lond 145:101–104

Journal : Small 10712 | Dispatch : 11-8-2017 | Pages : 34
Article No. : 9423 | ☐ LE | ☐ TYPESET
MS Code : GEOP-D-17-00046 | ☑ CP | ☑ DISK

Alley RB, Blankenship DD, Bentley CR (1987) Till beneath ice stream B. J Geophys Res 92(89):8921–8929

Amante C, Eakins BW (2009) ETOPO1 1 arc-minute global relief model: procedures, data sources and analysis. NOAA, Technical memorandum, NESDIS, NGDC-24

An M, Wiens DA, Zhao Y, Feng M, Nyblade AA, Kanao M, Li Y, Maggi A, Lévêque J-J (2015) S-velocitymodel and inferred Moho topography beneath the Antarctic Plate from Rayleigh waves. J Geophys Res Solid Earth 120:359–383

Anandakrishnan S, Blankenship DD, Alley RB, Stoffa PL (1998) Influence of subglacial geology on the position of a West Antarctica ice stream from seismic measurements. Nature 394:62–65

Bagherbandi M, Sjöberg LE (2012) Non-isostatic effects on crustal thickness: a study using CRUST2.0 in Fennoscandia. Phys Earth Planet Inter 200–201:37–44

Bagherbandi M, Tenzer R, Sjöberg LE, Novák P (2013) Improved global crustal thickness modeling based on the VMM isostatic model and non-isostatic gravity correction. J Geodyn 66:25–37

Bagherbandi M, Tenzer R, Abrehdary M, Sjöberg LE (2015) A New Fennoscandian crustal thickness model based on CRUST1.0 and gravimetric isostatic approach. Earth-Sci Rev 145:132–145

Bamber JL, Ferraccioli F, Joughin I, Shepherd T, Rippin DM, Sigert MJ, Vaughan DG (2006) East Antarctic ice stream tributary underlain by major sedimentary basin. Geology 34(1):33–36

Bannister S, Yu J, Leitner B, Kennett BLN (2003) Variations in crustal structure across the transition from West to East Antarctica Southern Victoria Land. Geophys J Int 155:870–884

Baranov A (2010) A new crustal model for Central and Southern Asia. Izvest Phys Solid Earth 46:34–46

Baranov A, Bobrov A (2017) The structure and properties of Archean cratons of the southern continents: similarities and differences. Russ Geol Geophys (in press)

Baranov A, Morelli A (2013) The Moho depth map of the Antarctica region. Tectonophysics 609:299–313

Bassin C, Laske G, Masters G (2000) The current limits of resolution for surface wave tomography in North America. EOS Trans AGU 81:F897

Behrendt JC, LeMasurier WE, Cooper AK, Tessensohn F, Trehu A, Damaske D (1991) Geophysical studies of the West Antarctic rift system. Tectonics 10(6):1257–1273

Bell RE, Blankenship DD, Finn CA, Morse DL, Scambos TA, Brozena JM, Hodge SM (1998) Influence of subglacial geology on the onset of a West Antarctic ice stream from aerogeophysical observations. Nature 394:58–62

Bentley CR, Ostenso NA (1962) On the paper of F.F. Evison, C.E. Ingram, R.H. Orr, and J.H. LeFort (1962) Thickness of the Earth's crust in Antarctica and surrounding oceans. Geophys J R Astron Soc 6:292–298

Bird P (2003) An updated digital model of plate boundaries. Geochem Geophys Geosyst 4(3):1027. doi:10.1029/2001GC000252

Blankenship D, Bentley C, Rooney ST, Alley RB (1986) Seismic measurements reveal a saturated porous layer beneath an active Antarctic ice stream. Nature 322:54–57

Blankenship D, Bell RE, Hodge SM, Brozena JM, Behrendt JC, Finn CA (1993) Active volcanism beneath the West Antarctic ice sheet and implications for ice-sheet stability. Nature 361:526–528

Block AE, Bell RE, Studinger M (2009) Antarctic crustal thickness from satellite gravity: implications for the Transantarctic and Gamburtsev Subglacial Mountains. Earth Planet Sci Lett 288(1–2):194–203

Bowin C, Scheer E, Smith W (1986) Depth estimates from ratio of gravity, geoid and gravity gradient anomalies. Geophysics 51(1):123–136

Brocher TM (2005) Empirical relations between elastic wavespeeds and density in the Earth's crust. Bull Seismol Soc Am 95(6):2081–2092

Cande SC, Stock JM, Müller RD, Ishihara T (2000) Cenozoic motion between East and West Antarctica. Nature 404:145–150

Chaput J, Aster RC, Huerta A, Sun X, Lloyd A, Wiens D, Nyblade A, Anandakrishnan S, Winberry JP, Wilson T (2014) The crustal thickness of West Antarctica. J Geophys Res Solid Earth. doi:10.1002/2013JB010642

Chen W, Tenzer R, Gu X (2014) Sediment stripping correction to marine gravity data. Mar Geod 37(4):419–439

Clow G, Cuffey K, Waddington E (2012) High heat-flow beneath the central portion of the West Antarctic ice sheet. Eos Trans AGU, Fall Meet. Suppl

Cutnell JD, Kenneth WJ (1995) Physics, 3rd edn. Wiley, New York

Dalziel IWD (1992) Antarctica: a tale of two supercontinents. Annu Rev Earth Planet Sci 20:501–526

Dalziel IWD, Elliot DH (1982) West Antarctica; problem child of Gondwanaland. Tectonics 1(1):3–19

Danesi S, Morelli A (2001) Structure of the upper mantle under the Antarctic Plate from surface wave tomography. Geophys Res Lett 28(23):4395–4398

Dewart GM, Toksoz MN (1965) Crustal structure in East Antarctica from surface wave dispersion. Geophys J R Astron Soc 10:127–139

Journal : Small 10712 Dispatch : 11-8-2017 Pages : 34
Article No. : 9423 LE TYPESET
MS Code : GEOP-D-17-00046 CP DISK

Eckhardt DH (1983) The gains of small circular, square and rectangular filters for surface waves on a sphere. Bull Géod 57:394–409

Eshagh M (2016) A theoretical discussion on Vening Meinesz-Moritz inverse problem of isostasy. Geophys J Int 207:1420–1431

Evison FF, Ingham CE, Orr RH, Le Fort JH (1960) Thickness of the earth's crust in Antarctica and the surrounding oceans. Geophys J 3:289–306

Fedorov LV, Grikurov GE, Kurinin RG, Masolov VN (1982) Crustal structure of the Lambert Glacier area from geophysical data. In: Craddock C (ed) Antarctic geoscience. Univ. of Wisconsin Press, Madison, pp 931–936

Ferraccioli F, Finn CA, Jordan TA, Bell RE, Anderson LM, Damaske D (2011) East Antarctic rifting triggers uplift of the Gamburtsev Mountains. Nature 479:388–392

Filina I, Blankenship D, Thoma M, Lukin VV, Masolov VN, Sen MK (2008) New 3D bathymetry and sediment distribution in Lake Vostok: implication for pre-glacial origin and numerical modeling of the internal processes within the lake. Earth Planet Sci Lett 276(1–2):106–114

Forsberg R, Olesen AV, Yidiz H, Tscherning CC (2011) Polar gravity fields from GOCE and airborne gravity. In: Proceedings of 4th international GOCE user workshop European Space Agency, ESA

Forsyth SW, Ehrenbarda RL, Chapin S (1987) Anomalous upper mantle beneath the Australian-Antarctic discordance. Earth Planet Sci Lett 84:471–478

Frederick BC, Young DA, Blankenship DD, Richter TG, Kempf SD, Ferraccioli F, Siegert MJ (2016) Distribution of subglacial sediments across the Wilkes Subglacial Basin, East Antarctica. J Geophys Res Earth Surf 121(4):790–813

Fretwell P, Pritchard HD, Vaughan DG, Bamber JL, Barrand NE, Bell R, Bianchi C, Bingham RG, Blankenship DD, Casassa G, Catania G, Callens D, Conway H, Cook AJ, Corr HFJ, Damaske D, Damm V, Ferraccioli F, Forsberg R, Fujita S, Gim Y, Gogineni P, Griggs JA, Hindmarsh RCA, Holmlund P, Holt JW, Jacobel RW, Jenkins A, Jokat W, Jordan T, King EC, Kohler J, Krabill W, Riger-Kusk M, Langley KA, Leitchenkov G, Leuschen C, Luyendyk BP, Matsuoka K, Mouginot J, Nitsche FO, Nogi Y, Nost OA, Popov SV, Rignot E, Rippin DM, Rivera A, Roberts J, Ross N, Siegert MJ, Smith AM, Steinhage D, Studinger M, Sun B, Tinto BK, Welch BC, Wilson D, Young DA, Xiangbin C, Zirizzotti A (2013) Bedmap2: improved ice bed, surface and thickness datasets for Antarctica. Cryosphere 7:375–393

Gladkikh V, Tenzer R (2011) A mathematical model of the global ocean saltwater density distribution. Pure Appl Geophys 169(1–2):249–257

Golynsky AV, Aleshkova ND (1997) Regional magnetic anomalies of the Weddell Sea Region and their geological significance. Polarforschung 67(3):101–117

Grad M, Guterch A, Janik T (1993) Seismic structure of the lithosphere across the zone of subducted Drake plate under the Antarctic plate, West Antarctica. Geophys J Int 115:586–600

Grad M, Tiira T, ESC Working Group (2009) The Moho depth map of the European Plate. Geophys J Int 176:279–292

Groenewald PB, Granham GG, Watkeys MK (1991) Geological evidence for a Proterozoic to Mesozoic link between southeastern Africa and Dronning Maud Land, Antarctica. J Geol Soc 148:1115–1123

Groushinsky AN, Groushinsky NP, Stroev PA, Yatsenko EV (1992) The Earth's crust in Antarctica and the effective relief of the continent. J Geodyn 15:223–228

Hansen S, Nyblade A, Pyle M, Wiens D, Anandakrishnan S (2009) Using S wave receiver functions to estimate crustal structure beneath ice sheets: an application to the Transantarctic Mountains and East Antarctic craton. Geochem Geophys Geosyst 10:Q08014

Hansen S, Nyblade A, Heeszel D, Wiens D, Shore P, Kanao M (2010) Crustal structure of the Gamburtsev Mountains, East Antarctica, from S-wave receiver functions and Rayleigh wave phase velocities. Earth Planet Sci Lett 300:395–401

Heiskanen WH, Moritz H (1967) Physical geodesy. Freeman W.H. and Co, San Francisco

Hinze WJ (2003) Bouguer reduction density, why 2.67? Geophysics 68(5):1559–1560

Hole MJ, LeMasurier WE (1994) Tectonic controls on the geochemical composition of Cenozoic alkali basalts from West Antarctica. Contrib Miner Petrol 117:187–202

Huebscher C, Jokat W, Miller H (1996) Structure and origin of southern Weddell Sea crust: results and implications. In: Storey BC, King EC, Livermore RA (eds) Weddell Sea tectonics and Gondwana break-up: Geology Society, London, Spec. Publ., vol 108, pp 201–212

Hungeling A, Tyssen F (1991) Reflection seismic measurements in western Neuschwabenland. In: Thornson MRA, Crame JA, Thomson JW (eds) Geological evolution of Antarctica. Proceedings of the fifth international symposium on Antarctic Earth Sciences, Robinson College, Cambridge, Cambridge University Press, Cambridge, UK, p 73

Journal : Small 10712 | Dispatch : 11-8-2017 | Pages : 34
Article No. : 9423 | LE | TYPESET
MS Code : GEOP-D-17-00046 | CP | DISK

Isanina E, Krupnova N, Popov S, Masolov V, Lukin V (2009) Deep structure of the Vostok Basin, East Antarctica as deduced from seismological observations. Geotektonika 3:45–50

Ito K, Ikami A (1986) Crustal structure of the Mizuho Plateau, East Antarctica, from geophysical data. J Geodyn 6:285–296

Jacobs J, Elburg M, Läufer AL, Kleinhanns IC, Henjes-Kunst F, Estrada S, Ruppel AS, Damaske D, Montero P, Bea F (2015) Two distinct Late Mesoproterozoic/Early Neoproterozoic basement provinces in central/eastern Dronning Maud Land, East Antarctica: the missing link, 15–21°E. Precamb Res 265:249–272

Johnson CL, Solomon SC, Head JW, Phillips RJ, Smith DE, Zuber MT (2000) Lithospheric loading by the north polar cap of Mars. Icarus 144:313–328

Jordan TA, Ferraccioli F, Vaughan DG, Holt JW, Corr H, Blankenship DD, Diehl TM (2010) Aerogravity evidence for major crustal thinning under the Pine Island Glacier region (West Antarctica). Geol Soc Am Bull 122:714–726

Jordan TA, Ferraccioli F, Armadillo E, Bozzo E (2013) Crustal architecture of the Wilkes Subglacial Basin in East Antarctica, as revealed from airborne gravity data. Tectonophysics 585:196–206

Kalberg T, Gohl K (2014) The crustal structure and tectonic development of the continental margin of the Amundsen Sea Embayment, West Antarctica: implications from geophysical data. Geophys J Int 198:327–341

Kanao M, Fujiwara A, Miyamachi H, Toda S, Tomura M, Ito K, Ikawa T (2011) Reflection imaging of the crust and the lithospheric mantle in the Lützow-Holm Complex, Eastern Dronning Maud Land, Antarctica, derived from the SEAL Transects. Tectonophysics 508:73–84

Karner GD, Studinger M, Bell RE (2005) Gravity anomalies of sedimentary basins and their mechanical implications: application to the Ross Sea basins, West Antarctica. Earth Planet Sci Lett 235:577–596

Kennett BLN, Engdahl ER, Buland R (1995) Constraints on seismic velocities in the earth from travel times. Geophys J Int 122:108–124

Kiele J, Marshall DL, Kyle PR, Kaminuma K, Shibuya K, Dibble RR (1983) Volcanic activity associated and seismicity of Mount Erebus 1982–1983. Antarct J US 18:41–44

Knopoff L, Vane G (1978) Age of East Antarctica from surface wave dispersion. Pure Appl Geophys 117:806–816

Kobayashi R, Zhao D (2004) Rayleigh wave group velocity distribution in the Antarctic region. Phys Earth Planet Int 141:167–181

Kogan A (1971) First experience in crustal investigation for Antarctica by deep seismic sounding. Russ J Geol Geophys 10:84–89 **(in Russian)**

Kogan AL (1972) Results of deep seismic soundings of the earth's crust in East Antarctica. In: Adie RJ (ed) Antarctic geology and geophysics. Universitetsforlag, Oslo, pp 485–489

Kolmakov AF, Mishenkin BP, Solovyev DS (1975) Deep seismic studies in East Antarctica. Bull Soviet Antarc Exped 5–15 (in Russian)

Kovach RL, Press F (1961) Surface wave dispersion and crustal structure in Antarctica and the surrounding oceans. Ann Geofis 14:211–224

Kudryavtzev G, Butzenko V, Kadmina I (1991) Crustal section across western Dronning Maud Land continental margin from geophysical data. In: Yoshida Y, Kaminuma K, Shiraishi K (eds) Proceedings of the sixth international symposium on Antarctic Earth Science, Abstracts. National Institute for Polar Research, Tokyo, pp 330–335

Laske G, Masters G, Ma Z, Pasyanos ME (2013) Update on CRUST1.0—A 1-degree global model of Earth's crust. Geophys Res Abstr 15:2658

Lawrence JF, Wiens DA, Nyblade A, Anandakrishnan S, Shore PJ, Voigt D (2006) Crust and upper mantle structure of the Transantarctic Mountains and surrounding regions from receiver functions, surface waves, and gravity: implications for uplift models. Geochem Geophys Geosyst 7

Leitchenkov G, Kudryavtzev G (1997) Structure and origin of the Earth's Crust in the Weddell Sea Embayment (beneath the Front of the Filehner and Ronne lee Shelves) from deep seismic sounding data. Polarforschung 67(3):143–154

Lloyd S, van der Lee S, França GS, Assumpção M, Feng M (2010) Moho map of South America from receiver functions and surface waves. J Geophys Res 115:B11315

Llubes M, Florsch N, Legresy B, Lemoine JM, Loyer S, Crossley D, Remy F (2003) Crustal thickness in Antarctica from CHAMP gravimetry. Earth Planet Sci Lett 212:103–117

Lythe MB, Vaughan DG, BEDMAP Consortium (2001) BEDMAP; a new ice thickness and subglacial topographic model of Antarctica. J Geophys Res B Solid Earth Planets 106(6):11335–11351

Marschall HR, Hawkesworth C, Leat PT (2013) Mesoproterozoic subduction under the eastern edge of the Kalahari-Grunehogna Craton preceding Rodinia assembly: the Ritscherflya detrital zircon record, Ahlmannryggen (Dronning Maud Land, Antarctica). Precamb Res 236:31–45

Journal : Small 10712 Dispatch : 11-8-2017 Pages : 34
Article No. : 9423 □ LE □ TYPESET
MS Code : GEOP-D-17-00046 ✔ CP ✔ DISK

Mayer-Gürr T, Rieser D, Höck E, Brockmann JM, Schuh W-D, Krasbutter I, Kusche J, Maier A, Krauss S, Hausleitner W, Baur O, Jäggi A, Meyer U, Prange L, Pail R, Fecher T, Gruber T (2012) The new combined satellite only model GOCO03s. Abstract submitted to GGHS2012, Venice

Mayer-Gürr T, Pail R, Gruber T, Fecher T, Rexer M, Schuh W-D, Kusche J, Brockmann J-M, Rieser D, Zehentner N, Kvas A, Klinger B, Baur O, Höck E, Krauss S, Jäggi A (2015) The combined satellite gravity field model GOCO05s. Presentation at EGU 2015, Vienna, April 2015

Mieth M, Jokat W (2014) New aeromagnetic view of the geological fabric of southern Dronning Maud Land and Coats Land, East Antarctica. Gondwana Res 25:358–367

Mishra D, Chandra Sekhar D, Raju V, Kumar V (1999) Crustal structure based on gravity–magnetic modeling constrained from seismic studies under Lambert Rift, Antarctica and Godavari and Mahanadi rifts, India and their interrelationship. Earth Planet Sci Lett 172:287–300

Molinari I, Morelli A (2011) EPcrust: a reference crustal model for the European Plate. Geophys J Int 185:352–364

AQ9 Mooney WD, Laske G, Masters TG (1998) CRUST 5.1: a global crustal model at $5° \times 5°$. J Geophys Res 103B:727–747

Morelli A, Danesi S (2004) Seismological imaging of the Antarctic continental lithosphere: a review. Glob Planet Change 42:155–165

Moritz H (1990) The figure of the Earth. Wichmann H., Karlsruhe, p 279

Moritz H (2000) Geodetic reference system 1980. J Geod 74:128162

Munson CG, Bentley CR (1992) The crustal structure beneath ice stream C and ridge BC, West Antarctica from a seismic refraction and gravity pro-file. In: Yoshida Y, Kaminuma K, Shiraishi K (eds) Recent progress in Antarctic earth science. TERRAPUB, Tokyo, pp 507–514

O'Donnell JP, Nyblade AA (2014) Antarctica's hypsometry and crustal thickness: implications for the origin of anomalous topography in East Antarctica. Earth Planet Sci Lett 388:143–155

Okal EA (1981) Intraplate seismicity of Antarctica and tectonic implications. Earth Planet Sci Lett 52:397–409

Oldenburg DW (1974) The inversion and interpretation of gravity anomalies. Geophysics 39(4):526–536

Pail R, Goiginger H, Schuh W-D, Höck E, Brockmann JM, Fecher T, Gruber T, Mayer-Gürr T, Kusche J, Jäggi A, Rieser D (2010) Combined satellite gravity field model GOCO01S derived from GOCE and GRACE. Geophys Res Lett 37:L20314

Pail R, Bruinsma S, Migliaccio F, Förste C, Goiginger H, Schuh W-D, Höck E, Reguzzoni M, Brockmann JM, Abrikosov O, Veicherts M, Fecher T, Mayrhofer R, Krasbutter I, Sansò F, Tscherning CC (2011a) First GOCE gravity field models derived by three different approaches. J Geod 85(11):819–843

Pail R, Goiginger H, Schuh WD, Höck E, Brockmann JM, Fecher T, Mayer-Gürr T, Kusche J, Jäggi A, Rieser D, Gruber T (2011b) Combination of GOCE data with complementary gravity field information (GOCO). In: Proceedings of 4th international GOCE user workshop, München

Parker RL (1972) The rapid calculation of potential anomalies. Geophys J R Astron Soc 31:447–455

Pratt JH (1855) On the attraction of the Himalaya Mountains, and of the elevated regions beyond them, upon the plumb-line in India. Philos Trans R Soc Lond 145:53–100

Ramirez C, Nyblade A, Hansen SE, Wiens DA, Anandakrishnan S, Aster RC, Huerta AD, Shore P, Wilson P (2016) Crustal and upper-mantle structure beneath ice-covered regions in Antarctica from *S*-wave receiver functions and implications for heat flow. Geophys J Int 204:1636–1648

Reading A (2004) The seismic structure of Wilkes Land/Terre Adelie, East Antarctica and comparison with Australia: first steps in reconstructing the deep lithosphere of Gondwana. Gondwana Res 7:21–30

Reading AM (2006) The seismic structure of Precambrian and early Paleozoic terranes in the Lambert Glacier region East Antarctica. Earth Planet Sci Lett 244:44–57

Reading A (2007) The seismicity of the Antarctic Plate, in Continental intraplate earthquakes: science, hazard and policy issues, edited by S. Stein and S. Mazzotti. Geol Soc Am Spec Pap 425:285–298

Reigber C, Lühr H, Schwintzer P (2002) CHAMP mission status. Adv Space Res 30:129–134

Ritzwoller MH, Shapiro NM, Levshin AL, Leahy GM (2001) Crustal and upper mantle structure beneath Antarctica and surrounding oceans. J Geophys Res B 106(12):30645–30670

Rodriguez E, Morris CS, Belz JE (2006) A global assessment of the SRTM performance: photogram. Eng Rem Sens 72(3):249–260

Rooney ST, Blankenship DD, Bentley CR (1987) Seismic refraction measurements of crustal structure in West Antarctica. In: McKenzie GD (ed) Gondwana Six: structure, tectonics and geophysics. Geophysical Monograph Series, vol 40. American Geophysical Union, Washington, DC, pp 1–7

Rouland D, Xu SH, Schindele F (1985) Upper mantle structure in the southeast Indian Ocean: a surface wave investigation. Tectonophysics 114:281–292

Roult G, Rouland D, Montagner JP (1994) Antarctica II: upper mantle structure from velocities and anisotropy. Phys Earth Planet Inter 84:33–57

Journal : Small 10712 Dispatch : 11-8-2017 Pages : 34
Article No. : 9423 LE TYPESET
MS Code : GEOP-D-17-00046 CP DISK

Sjöberg LE (2009) Solving Vening Meinesz-Moritz inverse problem in isostasy. Geophys J Int 179:1527–1536

Sjöberg LE (2013) On the isotactic gravity anomaly and disturbance and their applications to Vening Meinesz-Moritz gravimetric inverse problem. Geophys J Int 193(3):1277–1282

Smith AM, Jordan TA, Ferraccioli F, Bingham RG (2013) Influence of subglacial conditions on ice stream dynamics: seismic and potential field data from Pine Island Glacier, West Antarctica. J Geophys Res Solid Earth 118:1471–1482

Stagg HMJ, Colwel JB, Direen NG, O'Brien PE, Bernardel G, Borissova I, Brown BJ, Ishirara T (2004) Geology of the continental margin of Enderby and Mac. Robertson lands, East Antarctica: insights from a regional data set. Mar Geophys Res 25:183–219

Stonehouse B (2002) Encyclopedia of Antarctica and the Southern Oceans. Wiley, Chichester, p 391

Studinger M, Karner GD, Bell RE, Levin V, Raymond CA, Tikku AA (2003) Geophysical models for the tectonic framework of the Lake Vostok region East Antarctica. Earth Planet Sci Lett 216(4):663–677

Studinger M, Bell RE, Buck WR, Karner GD, Blankenship D (2004) Sub-ice geology inland of the Transantarctic Mountains in light of new aerogeophysical data. Earth Planet Sci Lett 220(3–4):391–408

Studinger M, Bell RE, Fitzgerald P, Buck WR (2006) Crustal architecture of the Transantarctic Mountains between the Scott and Reedy Glacier region and South Pole from aero-geophysical data. Earth Planet Sci Lett 250(1–2):182–199

Tapley BD, Bettadpur S, Watkins M, Reigber C (2004) The gravity recovery and climate experiment: mission overview and early results. Geophys Res Lett 31(9):L09607

ten Brink US, Hackney RI, Bannister S, Stern T, Makovsky Y (1997) Uplift of the Transantarctic Mountains and the bedrock beneath the East Antarctic ice sheet. J Geophys Res B 12:27603–27621

Tenzer R, Bagherbandi M (2012a) Reformulation of the Vening-Meinesz Moritz inverse problem of isostasy for isostatic gravity disturbances. Int J Geosci 3(5A):918–929

Tenzer R, Bagherbandi M (2012b) Reformulation of the Vening-Meinesz Moritz inverse problem of isostasy for isostatic gravity disturbances. Int J Geosci 3(5):918–929

Tenzer R, Gladkikh V (2014) Assessment of density variations of marine sediments with ocean and sediment depths. Sci World J 823296:9

Tenzer R, Hamayun, Vajda P (2009) Global maps of the CRUST2.0 crustal components stripped gravity disturbances. J Geophys Res 114, B, 05408

Tenzer R, Abdalla A, Vajda P, Hamayun (2010) The spherical harmonic representation of the gravitational field quantities generated by the ice density contrast. Contrib Geophys Geod 40(3):207–223

Tenzer R, Novák P, Gladkikh V (2011) On the accuracy of the bathymetry-generated gravitational field quantities for a depth-dependent seawater density distribution. Stud Geophys Geod 55(4):609–626

Tenzer R, Novák P, Vajda P, Gladkikh V, Hamayun (2012a) Spectral harmonic analysis and synthesis of Earth's crust gravity field. Comput Geosci 16(1):193–207

Tenzer R, Gladkikh V, Vajda P, Novák P (2012b) Spatial and spectral analysis of refined gravity data for modelling the crust-mantle interface and mantle-lithosphere structure. Surv Geophys 33(5):817–839

Tenzer R, Novák P, Gladkikh V (2012c) The bathymetric stripping corrections to gravity field quantities for a depth-dependent model of the seawater density. Mar Geod 35:198–220

Tenzer R, Chen W, Tsoulis D, Bagherbandi M, Sjöberg LE, Novák P, Jin S (2015) Analysis of the refined CRUST1.0 crustal model and its gravity field. Surv Geophys 36(1):139–165

Tenzer R, Bagherbandi M, Chen W, Sjöberg LE (2016) Global isostatic gravity maps from satellite missions and their applications in the lithospheric structure studies. IEEE J Select Top Appl Earth Obs Remote Sens 10(2):549–561

Trey H, Cooper A, Pellis G, della Vedova B, Cochrane G, Brancolini G, Makris J (1999) Transect across the West Antarctic rift system in the Ross Sea, Antarctica. Tectonophysics 301:61–74

Vening Meinesz FA (1931) Une nouvelle méthode pour la réduction isostatique régionale de l'intensité de la pesanteur. Bull Géod 29:33–51

von Frese RRB, Tan L, Kim JW, Bentley CR (1999) Antarctic crustal modeling from the spectral correlation of free-air gravity anomalies with the terrain. J Geophys Res 104:25275–25296

Watts AB (2001) Isostasy and flexure of the lithosphere. Cambridge University Press, Cambridge

Wiens D, Heeszel D, Sun X, Lloyd A, Nyblade A, Anandakrishnan S, Aster R, Chaput J, Huerta A, Wilson T (2012) New seismic structure models of Antarctica and implications for lateral changes in lithospheric thickness, mantle viscosity, and heat flow. In: Proceedings of SCAR conference, Portland, OR, USA

Wilson T, The POLENET Group (2011) The POLENET project: data acquisition status, initial results, future modeling. 11th International symposium on Antarctic Earth Sciences, Edinburgh, Scotland, 10–16 July

Journal : Small 10712 Dispatch : 11-8-2017 Pages : 34
Article No. : 9423 LE TYPESET
MS Code : GEOP-D-17-00046 CP DISK

Winberry JP, Anandakrishnan S (2003) Seismicity and neotectonics of West Antarctica. Geophys Res Lett 30:1931–1935

Winberry JP, Anandakrishnan S (2004) Crustal structure of the West Antarctic rift system and Marie Byrd Land hotspot. Geology 32:977–980

Wörner G (1999) Lithospheric dynamics and mantle sources of alkaline magmatism of the Cenozoic West Antarctic Rift system. Glob Planet Change 23:61–77

Zhu L, Kanamori H (2000) Moho depth variation in Southern California from teleseismic receiver functions. J Geophys Res 105:2969–2980

Journal : **10712**
Article : **9423**

Springer
the language of science

Author Query Form

Please ensure you fill out your response to the queries raised below and return this form along with your corrections

Dear Author

During the process of typesetting your article, the following queries have arisen. Please check your typeset proof carefully against the queries listed below and mark the necessary changes either directly on the proof/online grid or in the 'Author's response' area provided below

Query	Details Required	Author's Response
AQ1	Kindly check and confirm whether the corresponding author is correctly identified and amend if necessary.	
AQ2	Please check the edit made in the article title.	
AQ3	Journal instruction requires a city for affiliation; however, this is missing in affiliation [3]. Please verify whether the provided city is correct and amend if necessary.	
AQ4	Reference Bentley (1991) was mentioned in the manuscript; however, this was not included in the reference list. As a rule, all mentioned references should be present in the reference list. Please provide the reference details to be inserted in the reference list.	
AQ5	Please suggest whether the phrase 'Vening Meinesz's inverse problem' can be changed to 'Vening Meinesz-Moritz's inverse problem' in the sentence 'Moritz (1990) generalized Vening Meinesz's … spherical approximation of the Earth' for consistency.	
AQ6	Both 'ETOPO1' and 'ETOPO1.0' are used inconsistently in the manuscript. Please check whether this is appropriate.	
AQ7	Please suggest whether the phrase 'Filchner Ice Shelf' can be changed to 'Filchner-Ronne Ice Shelf' in Table 1 for consistency.	
AQ8	Please check whether the edit made in the sentence 'We computed the gravity disturbances … compute the gravity corrections' conveys the intended meaning.	

AQ9	References Groenewald et al. (1991) and Mooney et al. (1998) were provided in the reference list; however, these were not mentioned or cited in the manuscript. As a rule, if a citation is present in the text, then it should be present in the list. Please provide the location of where to insert the reference citation in the main body text.	